Locating Instability in the Lumbar Spine: Characterizing the Eigenvector

by

Samuel James Howarth

A thesis
presented to the University of Waterloo
in fulfillment of the
thesis requirement for the degree of
Master of Science
in
Kinesiology

Waterloo, Ontario, Canada, 2006

I hereby declare that I am the sole author of this thesis. This is a true copy of the thesis, including any required final revisions, as accepted by my examiners.

I understand that my thesis may be made electronically available to the public.

ABSTRACT

Overloading of the back can cause instability such that buttressing the instability is a primary objective of many of the leading edge therapeutic approaches. However, a challenge lies in determining the location of the instability or the least stable vertebral joint. A mathematical analysis, based on a commonly used approach in engineering for determining structural stability, has been developed for the lumbar spine. The purpose of this investigation was to determine the feasibility of a method for mathematically locating potential areas of instability within a computer-based model of the lumbar spine. To validate this method, the eigenvector from the stability analysis was compared to the output from a geometric equation that approximated individual vertebral joint rotational stiffness with the idea that the entry in the eigenvector with the largest absolute value would correspond to the vertebral joint and axis with the lowest stiffness. Validation of the eigenvector was not possible due to computational similarities between the stability analysis and the geometric rotational stiffness method. However, it has been previously demonstrated that the eigenvector can be useful for locating instability, and thus warrants future study. Determining the least stable vertebral joint and axis can be used to guide proper motor pattern training as a clinical intervention. It was also shown in this investigation that an even distribution of fascicle force and stiffness generated stability. This supports the idea that well-coordinated efforts of muscle activation are beneficial for improving stability of the lumbar spine.

ACKNOWLEDGEMENTS

Firstly, it is a pleasure to thank my supervisor Dr. Stuart McGill for his constant support, insights and mentorship during both my undergraduate and graduate education. I have definitely improved myself as both a researcher and a person as a result of Dr. McGill's guidance and tutelage. I also wish to acknowledge the contributions of my committee members Dr. Jack Callaghan and Dr. Richard Wells. Their suggestions and advice have proved extremely valuable during the course of this project, and throughout my education. I would also like to acknowledge the unending guidance of Janessa Drake and Steve Brown. I greatly appreciate their comments and insights and I consider myself lucky and privileged to work with such outstanding people. Lastly, but definitely not least, I would like to thank the financial support of the Natural Sciences and Engineering Research Council for funding my graduate studies for the past two years.

TABLE OF CONTENTS

LIST OF TABLES

LIST OF ILLUSTRATIONS

I. INTRODUCTION

Overloading of the back can cause instability such that buttressing the instability is a primary objective of many of the leading edge therapeutic approaches. It has been shown that the osteoligamentous lumbar spine will buckle at compressive loads near 90 N (Crisco et. al., 1992). The lumbar spine is routinely required to carry compressive loads far in excess of these tolerances. For example, the mass of the upper body, for an 80 kg person, will exert approximately 400 N of compressive load on the L4-L5 joint of the lumbar spine. This clearly illustrates the importance of the spine's musculature for improving the spine's ability to withstand compressive load without buckling. Moreover, it is important to locate the joints and rotational motions that could potentially lead to spinal instability so that appropriate motor patterns can be identified for improving the stability around a joint, and specifically around an axis that is considered to be weak in terms of stability.

Joint instability for the spine has been defined as abnormal motion patterns (Panjabi, 2003), or a loss of normal vertebral joint stiffness (Pope & Panjabi, 1985; McGill et. al., 2003). Physically, instability has been manifested as a temporary, abnormally large rotation about a single axis and at a single vertebral joint (McGill, 2001). These instabilities are either the result of previous injury to the spine that causes a reduction in vertebral joint stiffness (Oxland et. al., 1991) or can be the result of motor control errors that disturb the balance of muscle forces surrounding the spine (McGill et. al., 2003). Subsequently, lumbar spine stability is improved by appropriate coordination of muscle activation that produces muscle force and stiffness (McGill et. al., 2003). The ability of a muscle to influence the stability of the lumbar spine is

dependent on the posture and the externally applied load (Cholewicki & VanVliet, 2002) such that no single muscle is most important for improving the overall stability of the lumbar spine (Kavcic et. al., 2004). However, activation of particular muscles could be more beneficial for improving the stability around a particular rotational axis and at a given vertebral level that has been determined to be potentially unstable. The concept applied here is the symmetry of appropriate muscle stiffness influencing vertebral joint stiffness.

In vitro studies have investigated the hypothetical effect of muscles on the force/moment versus displacement/angle relationship by attaching wires, with a known tension, to functional spinal units (Kaigle et. al., 1995; Ulrich et. al., 1998). These studies provide a sufficient basis for illustrating the potential of muscles for improving the stability of the spine, but they do not give any indication of how spine stability is actively controlled, and they often lack a sufficient complement of muscles for adequately modeling the muscular potential for improving stability. Thus, mechanical models of the lumbar spine that include an analysis of stability are imperative for investigating the in vivo stabilizing effects of the spine's musculature. Based on mechanical principles of minimizing potential energy, these models provide instant insight into the in vivo quantification and control of lumbar spine stability (Cholewicki & McGill, 1996). Moreover, the theory of mechanical stability quantification allows for investigation of structural buckling configurations (Farshad, 1994). Crisco and Panjabi (1992) illustrated the process for determining the buckled configuration in the frontal plane for an osteoligamentous spine whereby the relative contributions of each vertebral joint to the final buckled configuration were given by the entries of the eigenvector associated with the smallest eigenvalue that was determined from the mathematical analysis of the lumbar

spine's stability. In order to determine the precise rotations at each vertebral level, the eigenvector was used as an initial guess to the system of five equilibrium equations defined from the first partial derivatives of the potential energy function. This method allows the investigators to locate potential areas of instability within their uni-planar osteoligamentous model of the lumbar spine.

1.1 Investigative Questions and Purpose

The purpose of this investigation is to validate a method for mathematically locating potential areas of instability within the in vivo lumbar spine. Given the ability of the eigenvector for locating potential instability in a uni-planar osteoligamentous model of the lumbar spine (Crisco & Panjabi, 1992), the questions to be answered by this investigation are:

1. Can the use of the eigenvector associated with the smallest eigenvalue be extended to locating potential lumbar spine instability in a three dimensional model of the lumbar spine with a full complement of active muscles?
2. What are the characteristics of motor patterns that improve stability?

1.2 Hypotheses

Although the eigenvector may not indicate the exact rotations at each joint, it does provide a measure of the relative contributions of each degree of freedom (a single joint and axis pair) to the final buckled configuration. Thus, it is hypothesized that:

1. The absolute value of the largest component of the eigenvector will indicate the degree of freedom that is least stable.
2. The stability of the system will depend on the coordination of muscle fascicle activation.

II. REVIEW OF LITERATURE

2.1 Clinical Determination of Instability and Biological Factors that Influence Spine Stability

Clinically spinal instability has been defined in previous work as either a loss of joint stiffness (Pope & Panjabi, 1985; McGill et. al., 2003), excessive range of motion (Posner et. al., 1982; Farfan & Gracovetsky, 1984), or as abnormal motion patterns (Panjabi, 2003). All three of these classifications imply that the vertebral joint has somehow been compromised in order for instability to occur (Oxland et. al., 1991). However, McGill and colleagues (2003) have noted that instability can be both the result and cause of injury. Stokes and Gardner-Morse (1995) noted that injury to the spine could be caused by inappropriate muscle activation patterns. For example, Cholewicki and McGill (1992) observed the excessive rotation of a single vertebral level during a competitive lift from an experienced power lifter. This excessive rotation has been classified as a temporary instability (McGill, 2001), and was likely the result of a motor control error. The lifter experienced pain in their lower back causing them to drop the weight. However, the lifter returned to lifting following this episode. Prior to this episode, the lifter had not experienced any injuries to their spine, and was in good health. The majority of the literature that focuses on the clinical definitions previously presented quantified instability of the lumbar spine as a function of injury.

2.1.1 In Vitro Quantification of Instability Using Osteoligamentous Lumbar Spines

Early in vitro studies quantified instability of functional spinal units (FSU's) as excessive range of motion (ROM) (Posner et. al., 1982). The ROM criteria from this study were used to develop a clinical checklist for detecting instability in patients. Panjabi (2003) gives an example of a clinical checklist for detecting instability. Their clinical criteria include displacement and rotational ROM limits as observed from sagittal plane radiographs under full flexion/extension. For the purposes of in vitro research a new measure termed the "neutral zone" (NZ) was defined (Panjabi et. al., 1989), and has been shown to be a better indicator of spinal instability onset (Oxland & Panjabi, 1992). It is important to note that these investigations were performed without applying a compressive preload to the specimen prior to testing. Applying this compressive preload would act to increase the stiffness of the specimen being tested. Specifically, the NZ is the residual displacement/rotation from the neutral position when no load is applied to the FSU (Panjabi et. al., 1989). However, it has been noted that the definition of the NZ is arbitrary (Scannell & McGill, 2003). In this light, the NZ is less formally defined as the portion of the moment-angle curve where large displacements occur with minimal applied load (ie. region of low stiffness) (Panjabi, 2003). The less formal definition of the NZ provides a picture of the vertebral joint's increased laxity following injury (Oxland & Panjabi, 1992). Typically, in vitro instability testing involves determining the force-displacement relationship of intact FSU's, and subsequently determining the force-displacement relationship of the FSU following serial sectioning of the passive elements surrounding the intervertebral joint. This method of "injuring" the spine is not an adequate representation of how injury to the tissues surrounding the spine occurs. Nonetheless this

testing method does yield an impression of the effects that sectioning various tissues has on the force-displacement relationship and more importantly the mechanical stiffness in both rotational and translational modes. A novel testing approach by Oxland and colleagues (1991) artificially created injuries to the spine by dropping a known mass from a known height onto the mounted FSU. Rapid compressive loading was performed as an attempt to generate burst fractures. Using a similar protocol to document the initiation and progression of spinal injury, Panjabi et al (1998) showed that the NZ increased as the injury's severity increased. Crisco and Panjabi (1992) documented the buckling load and relative vertebral rotations for whole osteoligamentous spines under the conditions of an uninjured spine, compromised facets, and compromised disc for applied compressive loads. Their results showed that injury to the disc and facets reduced the critical buckling load. The primary conclusion from this study was that injury to the spine was associated with a loss of stiffness that subsequently reduced the stability of the lumbar spine.

2.1.2 In Vitro Quantification of Instability with Simulated Muscle Forces

In vitro studies have focused on documenting the force-displacement relationship, and subsequent stability for a completely passive spine (Posner et. al., 1982; Oxland et. al., 1991; Oxland & Panjabi, 1992). Bergmark (1989) introduced the mechanical importance of the surrounding musculature, for improving the stability of the lumbar spine. In this work, he formalized the ability of the muscles to improve spine stability through the coordination of muscle force and stiffness. While Bergmark's (1989) formalism was purely theoretical, other researchers have attempted to document the effect of simulated muscle forces on the in vitro

stability of the lumbar spine FSU's (Panjabi et. al., 1989; Wilke et. al., 1995; Ulrich et. al., 1998).

Muscle forces are simulated by attaching cables to the FSU that pull from the anatomical origin or insertion points of the actual muscles, and along a similar line of action (ie. tangent to the direction of muscle pull from the point of attachment). The general conclusion from these studies is that muscle force and/or stiffness improves the stability of the lumbar spine. While these studies come to similar conclusions, the measures used for indicating instability are somewhat different. Panjabi et al (1989) showed that the NZ decreased with simulated muscle force when compared to loading situations with no added muscle forces. Moreover, Panjabi and colleagues (1989) argued that the proximity of the deeper, and smaller, muscles to the joint center of rotation would make them likely candidates for stabilizing the spine while the larger muscles that are further from the spine were used for moment generation. Ulrich et al (1998) found that L4-L5 ROM was reduced following muscle activation. Interestingly, this result was only observed for ROM in both lateral bend and axial rotation. These authors observed an increase in flexion/extension ROM when a similar moment was applied to the FSU. One possible explanation for this result could be a difference in moment arm lengths between the anterior (psoas), and posterior (multifidus) muscles. The investigators attempted to control the simulated muscle force. Thus, any differences in the moment arm lengths would create an unbalanced muscle moment that would subsequently lead to an increased flexion/extension ROM when the external moment was applied.

2.1.3 In Vivo Stabilizing Effects of Muscle Force and Muscle Stiffness

The previous in vitro results indicated that the musculature surrounding the spine was important for improving lumbar spine stiffness. Several in vivo investigations have been conducted to determine how the motor control system recruits muscles under different loading conditions, and different conditions of stability. Callaghan and McGill (1995) postulated that the recruitment of muscles under different loading condition was not aimed towards minimizing joint loading, and instead was directed towards improving spine stability. Firstly, it has been shown that as the load placed on the spine increases, muscle activation increases, and subsequently the stability of the spine increases (Cholewicki et. al., 2000). Furthermore, Granata and Orishimo (2001) demonstrated that increasing the potential energy of an externally applied load while maintaining a constant externally applied load caused cocontraction of the spine flexors and extensors to increase. For this investigation, the authors maintained the mass of the externally applied force, and the horizontal distance from the participant while varying the vertical height of the mass. This ensured that the moment about L4-L5 was equal in all cases while the potential energy of the external mass was allowed to increase. The increase in abdominal activity with increasing load height was deemed to improve the stability of the spine while the increased activation of the lumbar extensor muscles counteracted the net flexor muscle moment generated by the abdominal muscle activation (Granata & Orishimo, 2001). The cocontraction response of the motor control system has been shown to be advantageous in conditions with a low externally applied moment (Granata & Marras, 2000). The results of this investigation showed, through the use of a simplified mathematical model of the lumbar spine, that cocontraction of the musculature surrounding the

spine produced an increase in the maximum compressive load that could be applied to the spine without buckling. Furthermore, the beneficial effect of increased stability outweighed the deleterious effect of added compressive load from the muscle coactivation. The beneficial stabilizing effect of cocontraction has been postulated as an explanation for the increased cocontraction observed during lifting tasks in patients diagnosed with instability when compared to controls (Van Dieen et. al., 2003). In this regard, people with instability (or loss of joint stiffness) will compensate for compromised passive joint stiffness by increasing the active joint stiffness controlled by the musculature. The ability of muscle coactivation for improving the stability of the spine is elegantly explained by the analogy of adding compressive load to a fishing rod with and without supporting guy-wires (McGill, 2002). In this analogy, a fishing rod stood on its butt end, without additional support, will buckle almost immediately following application of compressive load to its tip. Addition of guy-wires arranged symmetrically about the rod's longitudinal axis, with equivalent force and stiffness characteristics allows the rod to buckle at a much higher applied compressive load. In addition, the ability of the rod with guy-wires to accept compressive load is compromised if there is an imbalance in the force and/or stiffness of one of the guy-wires. Thus, while the muscles can improve the stability of the lumbar spine through activation that generates muscle force and stiffness, it has been hypothesized that motor control errors resulting in a temporary loss of stiffness in a single degree of freedom could cause lumbar spine instability in a static instant (Cholewicki & McGill, 1992; Gardner-Morse et. al., 1995). Furthermore, these motor control errors allow the spine to remain in equilibrium, but can cause instability (Gardner-Morse et. al., 1995).

2.1.4 Optimal Improvements in Spine Stability with Muscle Activation

Another issue of importance in rehabilitating the unstable spine is to determine the motor patterns that are most beneficial for restoration of functional spine stability. Specifically, identifying the motor patterns that improve the stability of the lumbar spine while allowing the patient to functionally carry out daily activities explains the concept of "sufficient stability" (McGill, 2001). Common therapeutic approaches for rehabilitating the unstable spine have attempted to focus on activating specific muscles that have been identified as being "stabilizers". In particular, the approach of the Queensland group advocates activating the transversus abdominis for improving the stability of the lumbar spine (Hodges & Richardson, 1997). Recent research has shown that there is not one single muscle that is most important for improving the stability of the lumbar spine (Kavcic et. al., 2004). In particular, the ability of a given muscle to influence the stability of the lumbar spine is highly dependent on body posture and the external loading condition (Cholewicki & VanVliet, 2002).

2.1.5 Influences of Intra-abdominal Pressure on Spine Stability

Another means for improving spine stability in vivo is through intra-abdominal pressure (IAP). Cholewicki and colleagues (1999) used a physical model to simulate the effects that IAP can have on the stability of the lumbar spine. In their model, the muscles were represented by springs that stretched across the whole length of a column. The addition of a pneumatic piston mimicked the effect of IAP. The outcome of this study showed that the combination of muscle activation and IAP improved the stability of the lumbar spine. It has

been hypothesized that the stabilizing effect of IAP could be masked by the presence of abdominal muscle activation that accompanies generation of IAP (Cholewicki et. al., 1999). Namely, Callaghan and McGill (1995) observed an association between elevated IAP and increased abdominal muscle activity. Recently, Hodges et al (2005) conducted a study whereby the phrenic nerve was artificially stimulated in order to increase the intra-abdominal pressure in isolation from activation of the abdominal musculature. They tested the posteroanterior stiffness of the lumbar spine under the conditions of low IAP and elevated IAP to determine the effects that IAP might have on the spine's stiffness. A very small sample of participants was used for this investigation due to the invasive nature of recording IAP in vivo. Nonetheless, the results indicated that posteroanterior stiffness of the lumbar spine increased with the presence of IAP (Hodges et. al., 2005). The ability of IAP to increase the spine's stiffness independent of abdominal muscle activation indicates that IAP alone, along with the subsequent elastic stretch of surrounding tissues improves the stability of the lumbar spine. However, it remains to be shown whether this increase in stability is significant in the presence of abdominal muscle activity.

This section has outlined the importance of the different systems (active, passive) surrounding the spine for improving the stability of the lumbar spine. The musculature has the ability to improve the stability of the lumbar spine through properly coordinated patterns of muscle force and stiffness. Moreover, recruitment of the spine's musculature appears directed towards maintaining spine stability under various loading conditions.

2.2 Mechanical Computation of Spine Stability

2.2.1 The Energy Approach to Stability Computation – Mathematical Formalism and Pedagogical Analogy

A system is deemed to be mechanically stable if small changes in the system parameters or external loading conditions cause small changes to the existing physical state of the system (Farshad, 1994). Conversely, a system is deemed to be unstable if a large change in the existing physical state of the system occurs for a small change in the system parameters or external loading conditions (Farshad, 1994). The minimum potential energy approach to stability is a traditional method for determining the stability state of a system. More formally, Thompson and Hunt (1984) state, "a complete relative minimum of the potential energy with respect to the generalized coordinates is necessary and sufficient for the stability of an equilibrium state of the system". Mathematically, the condition for a local minimum is that the second variation of the potential energy function must be positive definite. Positive definiteness implies that all eigenvalues of the Hessian matrix for the potential energy function are greater than zero for the case of a system with n degrees of freedom ($n > 2$). Physically, the smallest eigenvalue represents the load at which the column will buckle (Farshad, 1994). Thus, buckling and instability occur when one or more of the eigenvalues becomes negative. For pedagogical purposes, the quantification of structural stability is best explained by the analogy of a ball rolling in a bowl (Figure 2.1).

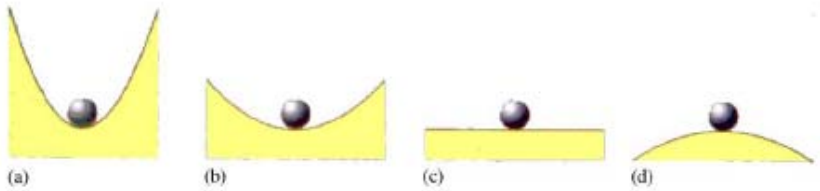

Figure 2.1 - The ball will move on the surface with an applied perturbation, and in the case of a ball in bowl (a, b), the ball's (gravitational) potential energy will increase. The ball's system is unstable if the energy given to the ball by the perturbation is sufficient to cause the ball to seek a new point of equilibrium by exiting the bowl. The surfaces indicated in (c) and (d) show systems that are in equilibrium, but are unstable. This is because once the ball is perturbed, it will not return to the same point.

This analogy is briefly explained here. McGill (2001) and Howarth and colleagues (2004) present a similar analogy that is specific to determination of lumbar spine stability.

The system is in a state of equilibrium when the ball is stationary and residing at the bottom of the bowl. The ball represents the equilibrium state of the system, and the bowl represents a two dimensional simplification of a complex potential energy surface. Application of an external force to a ball residing in the bottom of a bowl would cause the ball to move up the bowl's slope. The ball will return to its original equilibrium state (original position on the potential energy surface) if the applied load is insufficient to cause the ball to leave the bowl's local potential energy minimum. However, instability occurs if the applied perturbation is sufficient to cause the ball to leave its original local potential energy bowl. At this point, the ball will seek out a new local potential energy minimum under a new system configuration that is called the buckled configuration. It is also possible for the ball to initially reside at a maximum point on the potential energy surface. In this case, any applied perturbation will cause the ball to not return to its initial position on the potential energy surface.

2.2.2 Application of the Energy Approach for Computing Stability of the Lumbar Spine

Professor Anders Bergmark undertook the initial attempt for mechanically defining the stability of the lumbar spine in the late 1980's. This work outlined the conditions of minimum potential energy for maintenance of stable equilibrium using a three-dimensional model of the lumbar spine that comprised of 40 muscle fascicles, and representative passive properties (Bergmark, 1989). The concept of spine stability quantification, via the potential energy method, was extended by Cholewicki and McGill (1996). This model included a ribcage, pelvis, and the five intervening lumbar vertebrae as well as a set of 90 muscle fascicles (which has been updated to 118 with the bilateral addition of transversus abdominis), and a lumped passive parameter (McGill et. al., 1994) that included the stiffening effects of the ligaments, disc, and facets. While Bergmark (1989) had formulated individual muscle short-range stiffness as being proportional to the muscle force, and inversely proportional to its length $\left(k = q\frac{F}{L} \right)$, Cholewicki and McGill (1996) utilised a Distribution Moment (DM) model for deriving individual muscle force, and stiffness directly from measured electromyographic activity. This is significant since the value of q has been shown to be dependent on muscle activation and the ratio of tendon to muscle length (Cholewicki & McGill, 1995). This approximation to muscle stiffness is avoided by the DM model since it directly determines muscle stiffness from the muscle's assigned activation. However, the activation of some muscles is inferred from the measured activation of another muscle. For example, the activation for the modelled psoas muscle is derived from the internal oblique activation. Thus, some error in the muscle stiffness derivation using the DM model could be expected based on supposed muscle activities. Moreover, Cholewicki and McGill (1996) displayed the equations

whereby spine stability was determined from a sum of potential energies stored in the muscles, passive tissues, and the work done by an external load. Recent work by Brown and Potvin (2005) has demonstrated a geometrical method, based on a derived potential energy function, for the stability of a single lumbar joint (L4-L5) in two dimensions. The equations from this model were also used to derive an equation that determined the stabilizing potential of a muscle based on its attachment points and moment arm length to the instantaneous joint center of rotation (Potvin and Brown, 2005).

2.2.3 Stiffness Approach to Stability Computation Based on a Linearization of the Energy Method – Stability and Post-buckling Analyses

While the previous models focused on quantifying stability of the lumbar spine, they did not present a detailed mathematical account of the lumbar spine's post-buckling behaviour. Other attempts to quantify the mechanical stability of the lumbar spine have derived a stiffness-based approach that is a linearization of the equilibrium equations (first partial derivatives) of the lumbar spine's potential energy. Gardner-Morse and colleagues (1995) determined the critical value of the parameter *q* that would make the spine stable by solving the eigenproblem $(\mathbf{K_S} + \mathbf{K_M})\mathbf{v} + \lambda(\mathbf{G_S} + \mathbf{G_M})\mathbf{v} = \mathbf{0}$. The investigators indicated that the smallest positive eigenvalue (λ_{min}) indicated the stability of lumbar spine, and that its associated eigenvector (**v**) determined the buckling configuration. The matrices in the previous equation represent the global spine ($\mathbf{K_S}$) and muscle ($\mathbf{K_M}$) stiffness, as well as the geometric spine ($\mathbf{G_S}$) and muscle ($\mathbf{G_M}$) stiffness. It is important to note that the investigators determined the spine to be stable when $\lambda_{min} > 1$ while other classical analyses of mechanical stability consider a

system to be stable when $\lambda_{min} > 0$ (Thompson & Hunt, 1984). The authors present a figure (Figure 2.2) of the buckled configuration for the first three modes.

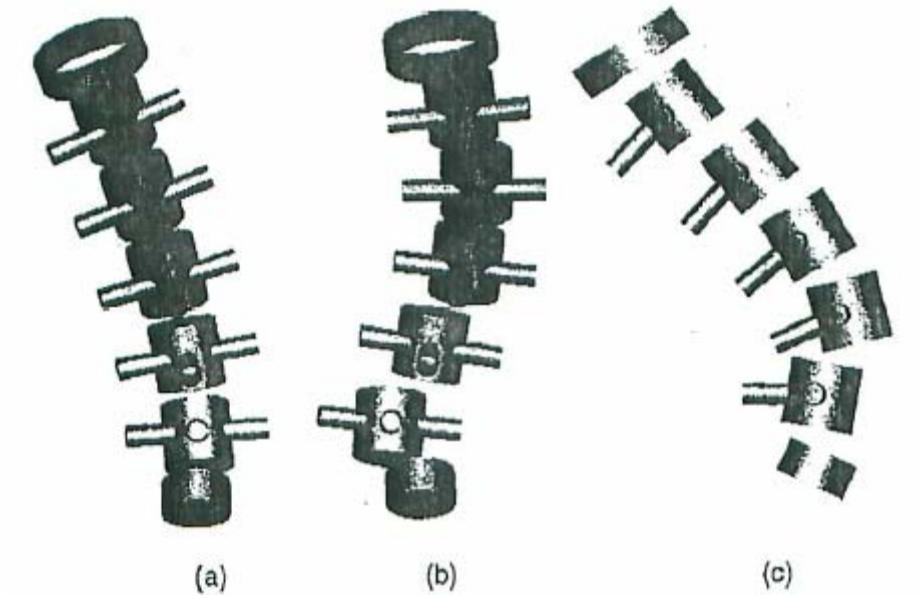

Figure 2.2 – The first three buckling modes of the lumbar spine as determined by eigenvectors (Reprinted with permission from Gardner-Morse et al, 1995).

These configurations are derived from the eigenvectors associated with the three lowest eigenvalues. However, no specific explanation is given of how the authors arrived at the final buckled configurations. A similar method was used by Crisco and Panjabi (1992) who developed a five degree of freedom model that determined the stability of the osteoligamentous lumbar spine under intact, compromised disc, and compromised facet conditions. The frontal plane (lateral bend) rotation at each vertebral joint in the lumbar spine was represented by a single degree of freedom in the mathematical model. Motion of the model was constrained to the frontal plane due to limitation in applying the theory of Euler column buckling to curved columns. In this manner, the model of the lumbar spine was constructed by arranging the vertebrae so that they formed a column in which, initially, the joint centers of rotation were

aligned vertically. Akin to the work of Gardner-Morse and colleagues (1995), the model of Crisco and Panjabi (1992) determined lumbar spine stability by solving the eigenproblem $\left(\mathbf{L}^{-1}\mathbf{K} - \lambda\mathbf{I}\right)\mathbf{v} = \mathbf{0}$ where $\mathbf{L}^{-1}$ is the inverse of a 5 x 5 matrix of vertebral lengths, **K** is a diagonal 5 x 5 stiffness matrix, λ are the eigenvalues, and **v** are the associated 5 x 1 eigenvectors. Again, the eigenvalues represented the critical buckling load, and the eigenvectors determined the buckled configurations in the frontal plane. The individual entries in the eigenvector associated with the smallest eigenvalue represented the relative contributions of each joint to the spine's buckled configuration. These relative contributions of each degree of freedom were used as an initial guess for a solution to the system of five equilibrium equations that would yield the precise vertebral rotations in the buckled configuration. The results from this study also showed that the eigenvector entries were sensitive to changes in vertebral joint rotational stiffness either through a compromised disc or facets. This result, and the interpretation of the 5 x 1 eigenvector in this model is similar to the interpretation of the entries for an 18 x 1 eigenvector determined from an 18 degree of freedom passive model of the lumbar spine (Howarth & McGill, 2005). The passive stiffness values for the work of Howarth & McGill (2005) were obtained from exponential curves fitted to moment-angle data collected in vivo while participants were harnessed jig that was free to float on a frictionless surface (McGill et al, 1994).

2.2.4 Simplified Models of Spine Stability for Quantitative Explanation of Biological Results

Other approaches to quantifying lumbar spine stability have utilised simplified models whereby the spine is treated as a rigid vertical column with a single degree of freedom

(Cholewicki et. al., 1999; Granata & Marras, 2000; Granata & Orishimo, 2001). The simplicity of these models allows for easy implementation. Such simple models are primarily used to provide insights to biologically observed phenomena, and not for direct, or precise computation of spine stability. For example, the work of Granata and Marras (2000) used the derivation of an equation for the stability of a simplified spine outfitted with springs and dampers that represented the flexor and extensor muscles of the spine for evaluating the benefits of antagonistic cocontraction. Similarly, Granata and Orishimo (2001) used a similar model for evaluating the effects of increasing the height of an externally applied load (ie. increasing potential energy of the external load) while maintaining the externally applied flexor moment (ie. identical mass and moment arm length). Likewise, Cholewicki and colleagues (1999) constructed a single degree of freedom model with springs to represent the flexor and extensor muscles, and a pneumatic piston to mimic the effects of intra-abdominal pressure on the ability of the column for accepting an applied compressive load prior to buckling. The results from these studies have been presented above in more detail. However, these studies illustrate the importance of simplified models of lumbar spine stability for providing insight into biologically observed or suspected results.

III. METHODS

3.1 – Overview of Methods

The feasibility of the eigenvector for locating the least stiff vertebral joint and axis was tested using set of carefully constructed muscle fascicles that were allowed to contribute active force and stiffness to the lumbar spine. The rotational stiffness at each vertebral joint and about the three axes (flexion/extension, lateral bend, axial rotation) were computed from the muscle geometry, force and stiffness and was compared to the entries of the eigenvector. Following the comparison, all instances of discrepancies between the eigenvector and geometric vertebral rotational joint stiffness methods were recorded and analysed. This overview is summarized in Figure 3.1.

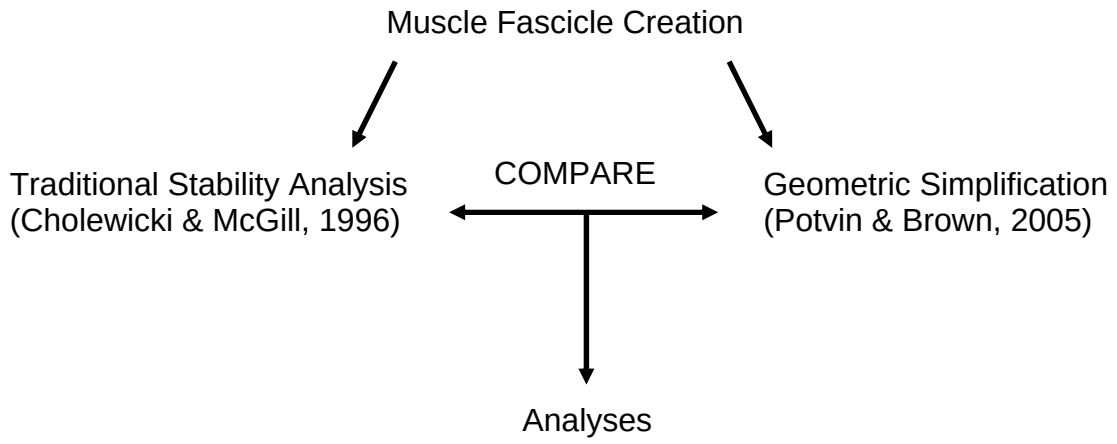

Figure 3.1 – A visual overview of the methods used for this investigation.

3.2 – Creation of Individual Muscle Fascicles for Actively Controlling Vertebral Joint Stiffness

3.2.1 – Grouping of Fascicles and General Attachment Point Locations

Artificial muscle fascicles were created to actively control the stiffness at each modeled lumbar vertebral joint. The muscle fascicles were grouped into bilateral artificial muscle fascicle pairs, and were divided into three categories; axis fascicles, quardrant fascicles, multisegmental fascicles. Axis and quadrant fascicles were created such that a single fascicle controlled stiffness at a single vertebral level. Hence these fascicles were called intersegmental muscle fascicles.

The following equation (1) demonstrates the general equation for determining the fascicle attachment locations in the case of an intersegmental fascicle (Figure 3.2).

$$\mathbf{a} = \mathbf{c} + s\mathbf{v} \quad (1)$$

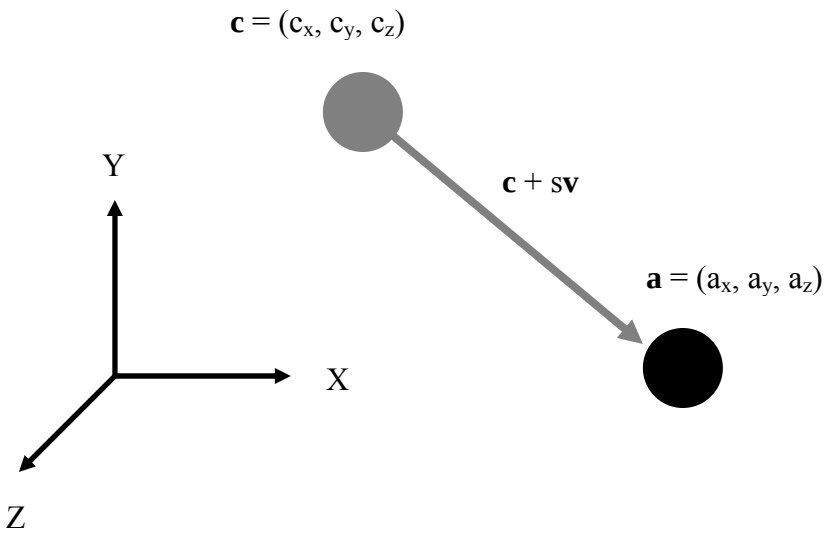

Figure 3.2 – Illustration of the terms in Equation (1). **a** is a fascicle attachment location, **c** is the vertebral joint center associated with the fascicle, **v** is a vector that defines the fascicle attachment location relative to the vertebral joint center, *s* is a scaling factor to control both the length and the moment arm length for each fascicle. The right handed coordinate system used in the model of the lumbar spine is defined by the X, Y and Z axes that respectively represent the lateral bend, axial rotation and flexion/extension axes.

The value of *s* was set to 0.025. It is important to note that the value of **v** in equation (1) will change depending on the attachment location. The different values for **v** are presented with the description of each set of intersegmental muscles (axis and quadrant). Moreover, the attachement locations for the multisegmental fascicles cannot be described using this exact formulation, but will be described in a later section.

3.2.2 – Orientation and Location of Axis Fascicles

Axis fascicles were placed and oriented such that they would contribute to the vertebral joint rotational stiffness of a single axis (either flexion/extension or lateral bend) at a single vertebral level. A total of 24 axis fascicles were modeled (6 joints x 4 fascicles per joint). At each vertebral joint, one fascicle pair was placed anteriorly and posterioly while the other fascicle pair was placed laterally relative to the vertebral joint center (Figure 3.3).

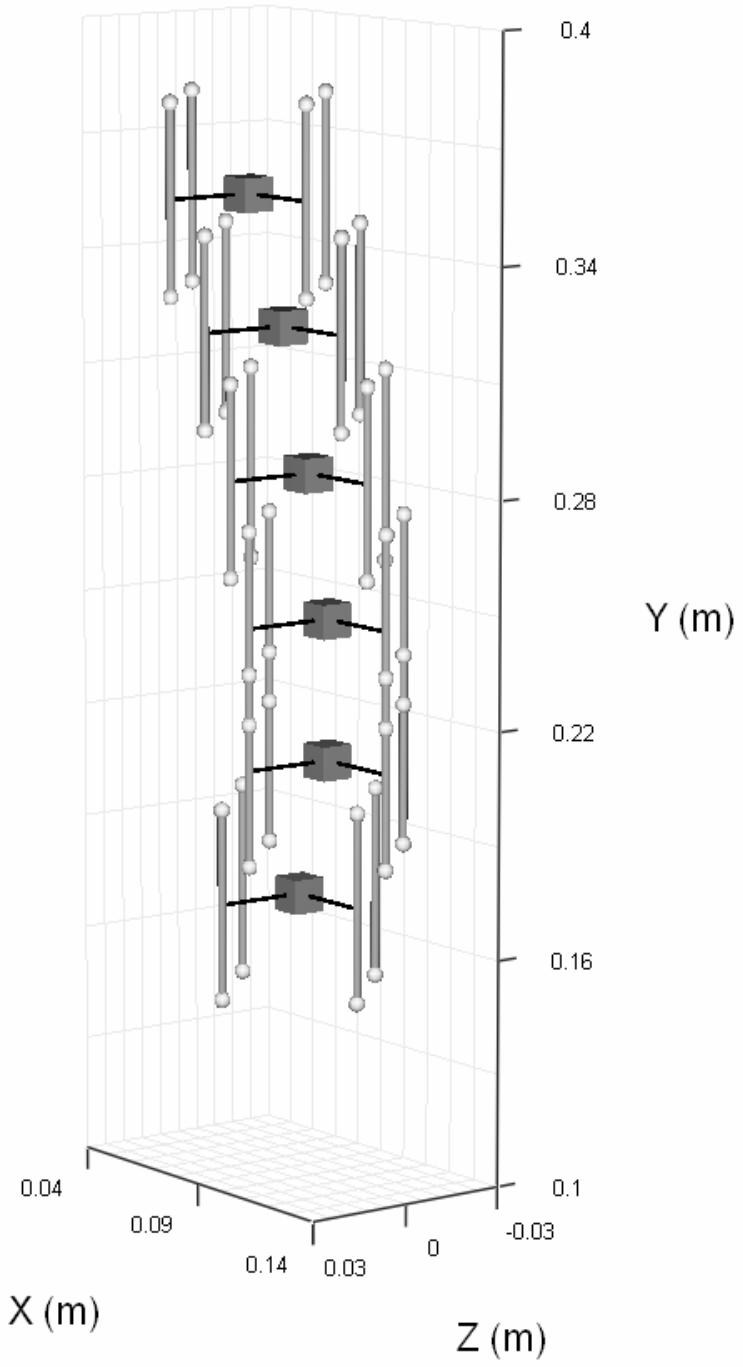

Figure 3.3 – The attachment locations for all axis fascicles. Vertebral joint centers are shown as the grey cubes with black lines indicating the positive X and Z axes at each vertebral joint. Muscle fascicle attachment locations are represented by light grey spheres.

The values for the attachment locations relative to each vertebral joint center (**v** in equation (1)) for the axis fascicles are listed below (Table 3.1).

Location	**v** Top Attachment	**v** Bottom Attachment
Anterior	(1,1,0)	(1,-1,0)
Posterior	(-1,1,0)	(-1,-1,0)
Left	(0,1,-1)	(0,-1,-1)
Right	(0,1,1)	(0,-1,1)

Table 3.1 – Locations of axis fascicle attachments relative to a vertebral joint center. These locations were applied to generate the attachment points for each set of axis fascicles surrounding a vertebral joint.

3.2.3 – Orientation and Location of Quadrant Fascicles

Quadrant fascicles were placed and oriented such that they contributed to the vertebral joint rotational stiffness about both of the flexion/extension and lateral bend axes at a single vertebral level. A total of 24 quadrant fascicles were modeled (6 joints x 4 fascicles per joint). At each vertebral joint, one fascicle pair was placed anteriorly on both sides of the vertebral joint center, and the other pair was placed posteriorly on both sides of the vertebral joint center (Figure 3.4).

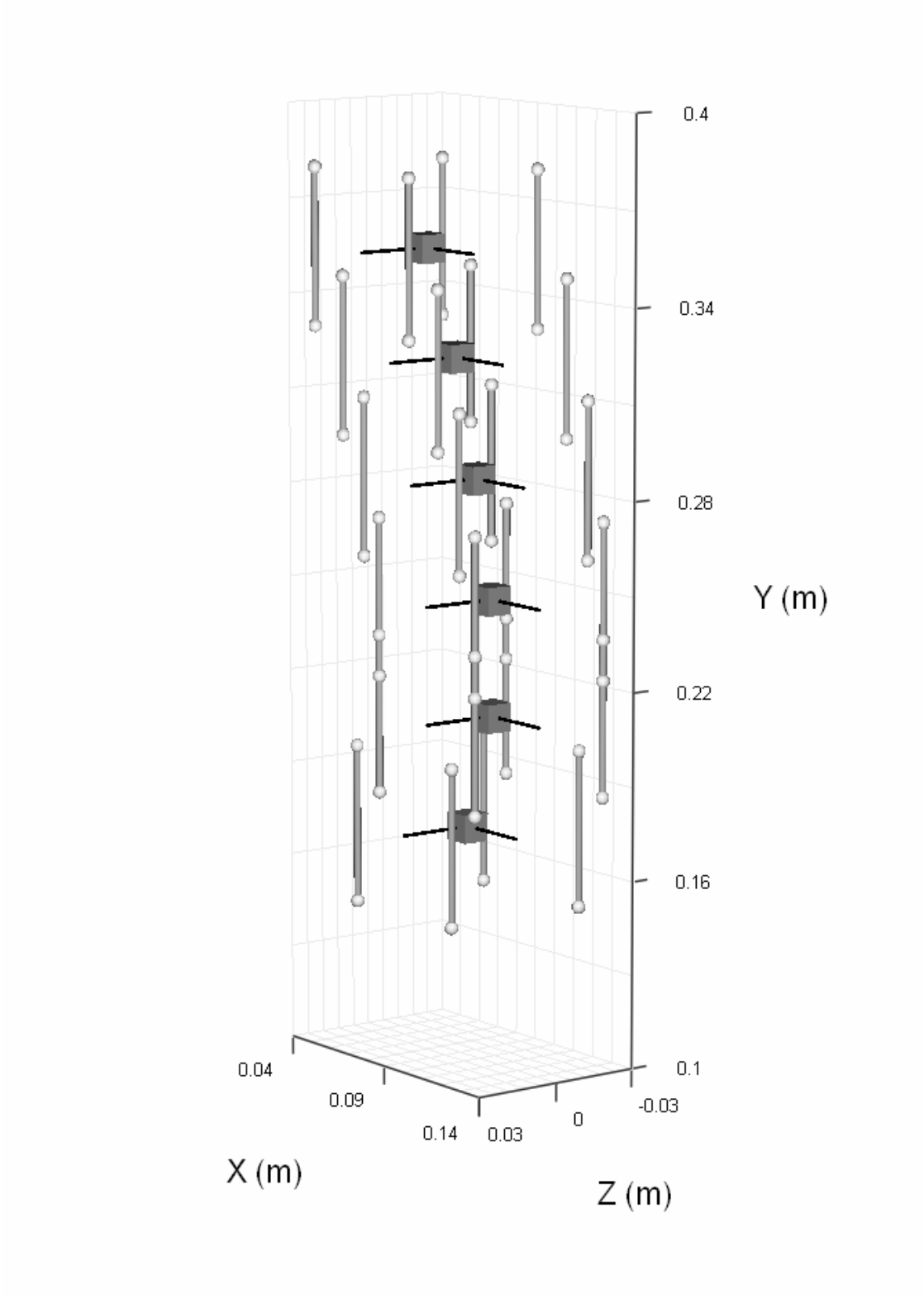

Figure 3.4 – The attachment locations for all quadrant fascicles. Vertebral joint centers are shown as the grey cubes with black lines indicating the positive X and Z axes at each vertebral joint. Muscle fascicle attachment locations are represented by light grey spheres.

The values for the attachment locations relative to each vertebral joint center (**v** in (1)) for the quadrant fascicles are listed below (Table 3.2).

Location	**v** Top Attachment	**v** Bottom Attachement
Anterior Right	(1,1,1)	(1,-1,1)
Anterior Left	(1,1,-1)	(1,-1,-1)
Posterior Right	(-1,1,-1)	(-1,-1,1)
Posterior Left	(-1,1,-1)	(-1,-1,-1)

Table 3.2 – Locations of quadrant fascicle attachments relative to a vertebral joint center. These locations were applied to generate the attachment points for each set of quadrant fascicles surrounding a vertebral joint.

3.2.4 – Orientation and Location of Multisegmental Fascicles

The multisegmental muscles were placed and oriented such that they contributed to the vertebral joint rotational stiffness about both of the flexion/extension and lateral bend axes at all of the modeled vertebral levels. A total of 4 multisegmental fascicles were modeled. Similar to the quadrant fascicles, one pair of multisegmental fascicles was placed anteriorly on both sides of the vertebral joint centers, and the other pair was placed posteriorly on both sides of the vertebral joint centers (Figure 3.5).

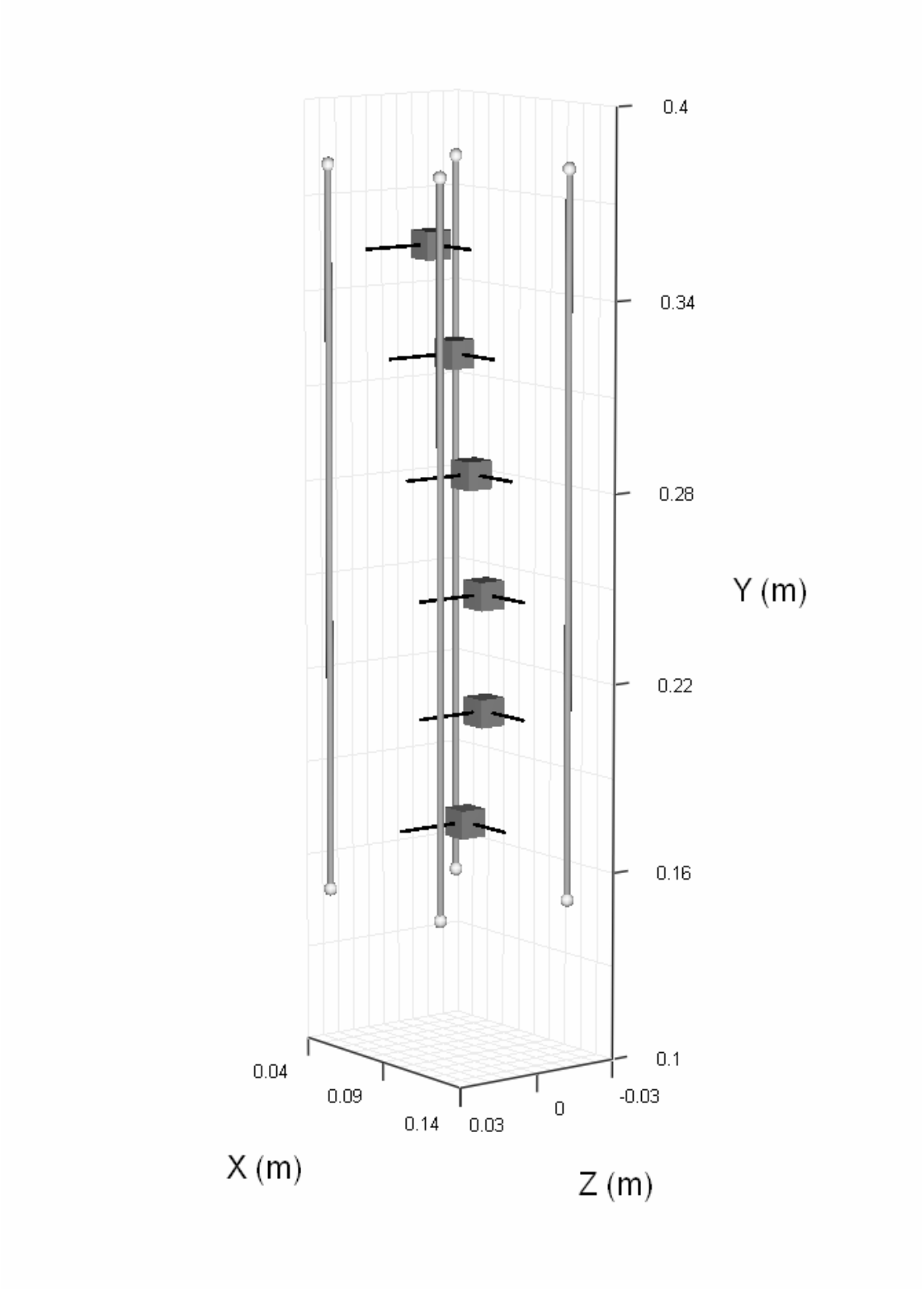

Figure 3.5 – The attachment locations for all multisegmental fascicles. Vertebral joint centers are shown as the grey cubes with black lines indicating the positive X and Z axes at each vertebral joint. Muscle fascicle attachment locations are represented by light grey spheres.

Unlike the intersegmental fascicles, the attachment locations of the multisegmental fascicles cannot be described by a single equation. However, the attachment coordinates for the multisegmental fascicles were derived in a similar manner by using combinations of individual vertebral joint center coordinates that pertained to the modeled Ribcage-L1 and L5-Pelvis joints (Table 3.3).

Location	Top Attachment	Bottom Attachment
Anterior Right	(P_x + 0.025, R_y + 0.025, 0.025)	(P_x + 0.025, P_y - 0.025, 0.025)
Anterior Left	(P_x + 0.025, R_y + 0.025, -0.025)	(P_x + 0.025, P_y - 0.025, -0.025)
Posterior Right	(R_x - 0.025, R_y + 0.025, 0.025)	(R_x - 0.025, P_y - 0.025, 0.025)
Posterior Left	(R_x - 0.025, R_y + 0.025, -0.025)	(R_x - 0.025, P_y - 0.025, -0.025)

Table 3.3 – Vertebral attachment locations for the multisegmental fascicles. The top attachments are made with the modeled ribcage and the bottom attachments are made with the modeled pelvis. P_x, P_y, R_x, R_y respectively are the X and Y coordinates of the Pelvis-L5 and Ribcage-L1 joints.

The multisegmental fascicles were also modeled in two different manners that were tested with separate simulations to determine the effects of modeling style on the computation of stability and determining the location of likely buckling. The first method modeled each multisegmental fascicle as a single segment that spanned from the ribcage to the pelvis. The second method utilised nodal points to break each multisegmental fascicle into a connected series of six segments of equal length. Equation (2) demonstrates the process for determining the location of the nodal points for a multisegmental muscle.

$$\mathbf{x_i} = \mathbf{b} + \frac{iL_m}{6}\frac{(\mathbf{a}-\mathbf{b})}{\|\mathbf{a}-\mathbf{b}\|} \quad (2)$$

Here $\mathbf{x_i}$ is the vector denoting the location of the i^{th} nodal point for fascicle m, $\mathbf{a}$ and $\mathbf{b}$ are the endpoint attachments for the multisegmental fascicle, L_m is the length of the fascicle between

the endpoints, i (i = 1, 2, 3, 4, 5) is an integer value indicating the nodal point number. Nodal points were utilised by Cholewicki and McGill (1996) to model the curvature of a muscle fascicle. Adding nodal points to the multisegmental fascicles modeled for this investigation may illustrate why discrepancies occur between the two computational procedures that are explained later.

3.3 – Muscle Fascicle Parameters

Each modeled fascicle (both intersegmental and multisegmental) was assigned a physiological cross-sectional area of 10 cm^2 to avoid differences in stiffness due to differences in physiological cross-sectional area. The length of each modeled fascicle was computed as the distance between fascicle attachment points (3).

$$L_m = \|\mathbf{a} - \mathbf{b}\| \quad (3)$$

Here L_m is the fascicle length, **a** and **b** are fascicle endpoint locations. The length of each intersegmental (both axis and quadrant) fascicle was 0.05 m, and the length of each multisegmental fascicle was 0.231 m. In the case when the multisegmental fascicles were modeled with nodal points, the length of each section was 0.0385 m (0.231 m per fascicle / 6 sections per fascicle).

For every iteration in each simulation, an activation value that ranged from 0 to 1 was assigned to each fascicle in order to produce active force and stiffness contributions to

mechanical stability. Each iteration involved randomly generating a total of 19 activation values that will be referred to as a motor pattern. Each pair of axis fascicles (either an anterior/posterior or lateral pair at a single vertebral joint) was randomly assigned identical activation values in order to maintain the assumption of balanced moments that is inherent in the mechanical computation of stability. Thus a total of 12 activation values were assigned to axis fascicles (6 joints x 2 axis pairs per joint) for each iteration. Each set of quadrant fascicles surrounding a vertebral joint, and the set of multisegmental fascicles were also randomly assigned identical activation values. Thus for the quadrant fascicles a total of 6 activation values were generated, and a single activation value was generated for the multisegmental fascicles for each iteration.

The randomly generated motor pattern of the current iteration was compared to the motor patterns of all previous iterations in the current simulation in order to eliminate the possibility of duplicate motor patterns. The current iteration was issued a new randomly generated motor pattern in the event of a duplicate motor pattern and the same comparisons were carried out until a novel randomly generated motor pattern was created.

Fascicle force and stiffness were computed following the assignment of an activation value. The active force for each fascicle was determined using the EMG to force model demonstrated by McGill and Norman (1986) and modified for use in this investigation (4).

$$F_m = \left(\frac{EMG_m}{MAXEMG_m} \right)^{1.3} A_m \quad (4)$$

Here F_m is the fascicle force, $\frac{EMG_m}{MAXEMG_m}$ is the normalized fascicle activation level, and A_m is the fascicle's physiological cross-sectional area. Subsequently, the stiffness of each fascicle was determined using the relationship between force and fascicle length presented by Bergmark (1989) (5).

$$k_m = q\frac{F_m}{L_m} \quad (5)$$

Here, k_m is the fascicle stiffness, F_m is the fascicle force, L_m is the current fascicle length, and q is a dimensionless proportionality constant. A nominal q value of 10 was used for this investigation which is consistent with the documented range of q values for skeletal muscle (Cholewicki & McGill, 1995), and has been used in a previous investigation (Potvin & Brown, 2005).

3.4 – Eigenvalue and Eigenvector Computation for Stability Analysis

An eigenvalue (λ) of a square matrix H is a real number that satisfies the following equation for a non-zero vector $\vec{x}$.

$$\mathbf{Hx} = \lambda\mathbf{x} \quad (6)$$

Any non-zero vector that satisfies this equation for a given eigenvalue is called an eigenvector associated with the eigenvalue λ. Alternatively this equation can be rewritten as a homogenous system.

$$(\mathbf{H} - \lambda\mathbf{I})\mathbf{x} = \mathbf{0} \quad (7)$$

In this case **I** is an identity matrix, where all the entries along the main diagonal are 1 and all other entries in the matrix are 0. Mathematically, solving for the eigenvalues of **H** requires the matrix $(\mathbf{H} - \lambda\mathbf{I})$ to be singular (ie. $\det(\mathbf{H} - \lambda\mathbf{I}) = 0$). Computing the determinant of this matrix produces a polynomial of an order that is equivalent to the dimension of **H** that is called the characteristic polynomial. The roots of this polynomial are the eigenvalues of the matrix **H**. Substituting an eigenvalue, λ, into (7), and solving (7) will produce an eigenvector associated with the eigenvalue λ. The eigenvector can then be normalized so that $\|\mathbf{x}\| = 1$.

For the purposes of lumbar spine stability computation, the matrix **H** in (6) and (7) is the Hessian matrix of the potential energy function. For our 18 dimensional model of the lumbar spine, the Hessian matrix is an 18 x 18 square, symmetric, and real-valued matrix of all possible second partial derivatives of the potential energy function (Cholewicki & McGill, 1996; Howarth et. al., 2004). The potential energy function for the analysis of lumbar spine stability is a summation of the contributions from the muscle fascicles, passive tissues, and the deleterious contribution from any externally applied load (8).

$$V = U_{muscle} + U_{passive} - W_{ext} \quad (8)$$

A complete description, and derivation of each term in (8), and the partial derivatives of (8) is given by Cholewicki and McGill (1996), and is reproduced here in Appendix A.

Since **H** is symmetric, and contains only real numbers, in the stability analysis, we are guaranteed a complete set of 18 real-valued eigenvalues. Each eigenvalue of the Hessian matrix represents the slope of the potential energy surface in a particular degree of freedom in the neighbourhood of a critical point (i.e. point where all first partial derivatives of the potential energy function are zero) (Thompson & Hunt, 1984). The eigenvalues and eigenvectors associated with the potential energy function's Hessian matrix were determined using the Matlab "eig" command.

[eVecs, eVals] = eig(Hessian)

This command returns the complete numerically ordered set of eigenvalues (in ascending order) in the variable eVals, and a matrix where the columns are the individual eigenvectors (eVecs). The order of the columns in eVecs is identical to the order of the eigenvalues in eVals (i.e. the first column in eVecs is the eigenvector associated with the first eigenvalue in eVals).

3.5 – Simplified Geometric Approach to Individual Joint and Axis Stability

The equation (9) from Potvin and Brown (2005) was used to determine the stabilizing potential of a given fascicle about a given axis at a vertebral joint that was spanned by the fascicle (Figure 3.6).

$$S_Z^m = F_m\left(\frac{a_X b_X + a_Y b_Y - r_Z^{\,2}}{l}\right) + k_m r_Z^{\,2}$$

$$r_Z = \frac{a_y b_x - a_x b_y}{l} \qquad (9)$$

$$l = \|\mathbf{a} - \mathbf{b}\|$$

$$\mathbf{a} = (a_x, a_y, a_z) \quad \mathbf{b} = (b_x, b_y, b_z)$$

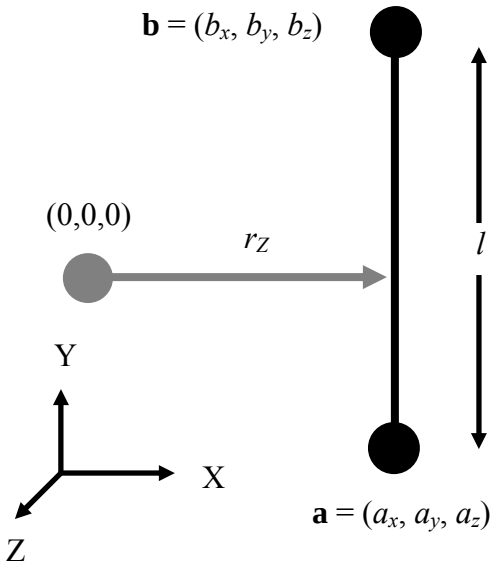

Figure 3.6 – Illustration of the geometrical parameters in the equation for determining the stabilizing potential of a fascicle at a particular vertebral joint and along a particular orthopaedic axis.

In this expression, S_Z^m is the contribution of fascicle *m* to stability about the Z-axis, **a** is the three dimensional vector of coordinates for the origin of fascicle *m*, **b** is the three dimensional vector of coordinates for the insertion of fascicle *m*, r_Z is the projection of the moment arm onto the Z-axis for fascicle *m*, l is the length of the fascicle *m* between **a** and **b**, F_m is the force supplied by fascicle *m*, k_m is the stiffness of fascicle *m*. Similar equations can be derived for the individual fascicle contributions to stability about the other two axes (X, Y).

The individual contributions, at each vertebral joint and about each of the three axes, for each fascicle that spanned the joint were added along with the passive and external load components from the relevant entries in the Hessian matrix (this is congruent with the method of Brown and Potvin, 2005) to yield the total contribution to stability at each vertebral joint and along each axis (10).

$$S_{Z,j} = \left(\sum_{i=1}^{M} S_Z^i \right) + \frac{\partial^2 U_T}{\partial \theta_{Z,j}{}^2} - \frac{\partial^2 W}{\partial \theta_{Z,j}{}^2} \quad (10)$$

Here, $S_{Z,j}$ is the stability including the contribution of all fascicles crossing a particular vertebral level and the passive tissues and external load, *M* is the total number of fascicles that cross that vertebral level. A similar equation can be developed for the stability about the other two axes (*X*, *Y*). This method is an approximation to the terms on the main diagonal of the Hessian matrix that is described in the previous section. Each of the stability values for each vertebral joint and each axis were organized according to the proposed form of the eigenvector that is explained in 3.7 to allow for comparisons.

3.6 – Simulation Conditions

The passive contribution about the axial twist axis was increased for computation of the terms in the Hessian matrix due to the lack of a fascicle (modeled in this investigation) that could independently control the stiffness about the axial twist axis for each vertebral joint. This eliminated the possibility that the axial twist axis for any vertebral joint would be the least stiff axis.

A series of simulations with differing degrees of complexity were run in order to test the feasibility of using the eigenvector for locating the most likely mode of buckling. Each simulation consisted of 10000 iterations with distinct randomly generated motor patterns. The following is a list of the simulations that were tested in this investigation.

1. Axis fascicles
2. Axis and quadrant fascicles
3. Axis, quadrant and multisegmental fascicles without nodal points
4. Axis quadrant and multisegmental fascicles without nodal points and vertebral joint centers aligned
5. Axis quadrant and multisegmental fascicles with nodal points
6. Axis quadrant and multisegmental fascicles with nodal points and vertebral joint centers aligned
7. Axis and multisegmental muscles without nodal points

Aligning the vertebral joint centers was performed in simulations 4.), and 6.), in order to test the assumption of a straight column for mechanical stability computation. Simulation 7.) was performed in order to allow for comparisons of the number of stable versus unstable cases between simulations 1.), 2.), and 3.).

3.7 – Comparison of Eigenvector with Individual Joint and Axis Stability

Crisco and Panjabi (1992) illustrated that each entry in the eigenvector associated with the smallest eigenvalue corresponded to the rotation at a given degree of freedom in their uniplanar model of the osteoligamentous lumbar spine. From the construction of the Hessian matrix for determining stability, Howarth and McGill (2005) have proposed a similar form of the 18 dimensional eigenvector associated with the smallest eigenvalue (Figure 3.7).

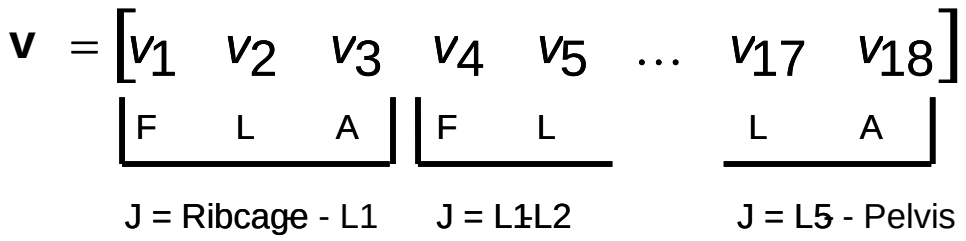

Figure 3.7 – In the proposed form of the eigenvector, each entry is associated with a particular joint and axis in the model of the lumbar spine.

Here, **v** is the eigenvector associated with the smallest eigenvalue. The entries v_i (i = 1…18) are the individual eigenvector entries. F/L/A are flexion-extension/lateral bend/axial rotational degrees of freedom at a single joint given by J. Again, the magnitude of each eigenvector entry

is related to a rotation about a particular axis at a specific vertebral joint in the 18 dimensional model of the lumbar spine.

It has been demonstrated that the least stable joint and axis combination in the modeled osteoligamentous lumbar spine is represented by the largest absolute value in the eigenvector (Crisco & Panjabi, 1992; Howarth & McGill, 2005). In order to determine the ability of the eigenvector for locating potential instability in the modeled lumbar spine with muscle fascicles, the proposed form of the eigenvector was compared to the individual joint and axis stability values obtained from the equation of Potvin and Brown (2005). The comparison for every iteration began by finding the index (an integer value between 1 and 18) of the eigenvector entry with the largest absolute value, and subsequently determining the index of the smallest value computed using Potvin and Brown's equation. The two indices were compared for every iteration, the motor patterns, smallest eigenvalue, absolute value of the eigenvector entries, outputs from Potvin and Brown's equation, and the indices from each computational method were recorded when a discrepancy between the two indices occurred.

3.8 – Comparison Analyses

The number of discrepancies for each set of 1000 iterations (thus each simulation was broken into 10 subsets of 1000 iterations) were recorded in order to demonstrate the randomness of the motor pattern generation, and to allow for statistical comparison between the different simulation conditions (this was only done for the first six simulations because the last simulation was added to allow for a different comparison that will be explained later). The likelihood of a discrepancy between the indices predicted by both methods for each vertebral joint and axis combination was also compiled for simulations 1.), 2.), 3.), 5.) in order to test if discrepancies were biased towards particular vertebral joint and axis combinations. When a discrepancy occurred, the different joint and axis combination predicted by the equation of Potvin and Brown (2005) was recorded to determine the distribution of discrepancies across the different joint and axis combinations.

A separate analysis was performed to determine the conditions for generating a stable case in the first simulation with only axis fascicles. The range of fascicle activation for each axis (flexion/extension and lateral bend), across all the modeled vertebral joints was recorded for each iteration. Iterations were grouped according to whether the motor pattern generated a stable or an unstable case as indicated by the smallest eigenvalue.

3.9 – Statistical analyses

Differences in the likelihood of a discrepancy occurring for each simulation were tested with a one way analysis of variance (ANOVA). Tukey's HSD post hoc test was used to identify the differences for this analyses. Two T-tests with unequal sample sizes and unequal variances were run to compare the range of fascicle activation between the stable and unstable cases in the simulation with only axis fascicles. Statistical differences were accepted as significant when $p < 0.05$.

IV. RESULTS

4.1 – Comparison Between Eigenvector and Simplified Geometric Approach (Simulation Analysis)

The traditional model for computing lumbar spine stability and the simplified geometric computational approach predicted the same location of likely buckling in 99.21% and 99.22% of the instantiations respectively for the simulation with only axis fascicles and the simulation with the combined axis and quadrant fascicles (i.e. simulations where the fascicles were oriented so that they spanned a single joint) (Figure 4.1). The addition of multisegmental fascicles to the model significantly increased the likelihood that the two models would not predict the identical degree of freedom as being the most likely to buckle (Figure 4.1, $p < 0.0001$). The matching between the two models improved after adding nodal points to the multisegmental fascicles, and running the same set of motor patterns that were run for the simulation containing multisegmental fascicles without nodal points. Adding nodal points to the multisegmental fascicles reduced the likelihood of non-matching between the two models relative to the simulation with multisegmental muscles without nodal points ($p < 0.0001$), but was not successful in creating identical or similar likelihoods of matching between the two models as in the cases with only intersegmental fascicles (Figure 4.1, $p < 0.0001$). Aligning the vertebral joint centers into a vertical column had no effect on the outputs of either model in the case with the complete set of intersegmental and multisegmental fascicles (Figure 4.1).

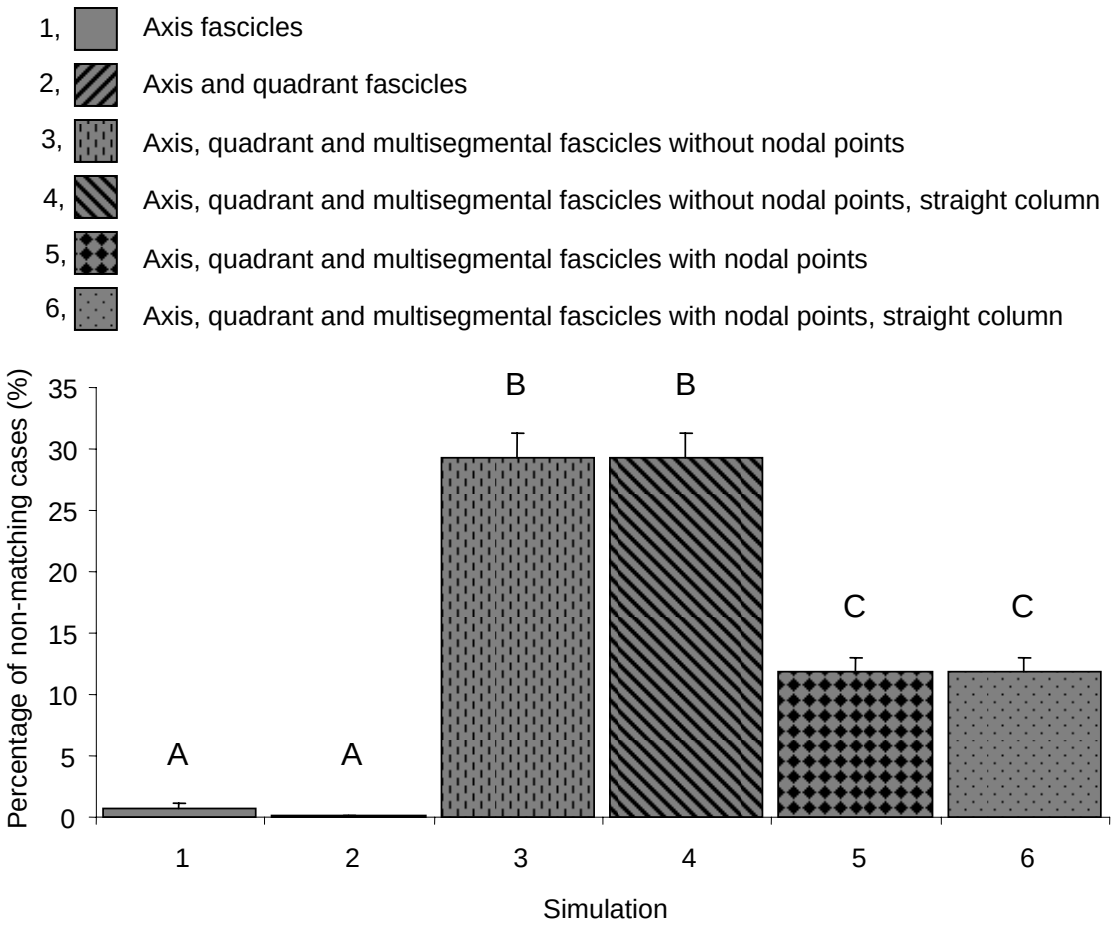

Figure 4.1 – The percentage (100% = 10000 iterations) of iterations where the index of the eigenvector entry with the largest absolute value did not match the index with the highest computed stability from the simplified geometrical approach. The legend above the graph indicates the set of fascicles that were used for the different simulations. Means with the same letter are not statistically different. Different letters indicate statistical differences between means ($p < 0.0001$).

The muscle fascicles were constructed to span a single vertebral joint, and were oriented so that they controlled the stiffness at a single (axis) or two (quadrant) rotational degrees of freedom at a given vertebral joint. The traditional stability analysis employed by Cholewicki & McGill (1996) and the simplified geometric approach of Potvin and Brown (2005) both use vectors connecting vertebral joint centers to the fascicle attachments during their computations. In the case with only intersegmental fascicles, the set of vectors connecting

vertebral joint centers is identical for both methods. However, the introduction of multisegmental fascicles creates a difference in this set of vectors between the two computational approaches and reduces the likelihood that the eigenvector and the simplified geometrical approach would predict the same vertebral joint and axis as being the least stable. The computation employed by Cholewicki & McGill (1996) in the case of multisegmental fascicles without nodal points uses two vectors (one for each of the upper and lower attachment locations) that connects the vertebral joint center at the level of the attachment to the attachment location for computation of the fascicles contribution to stability at all joints spanned by the fascicle (Figure 4.2). Conversely, the method employed by Potvin & Brown (2005) considers a set of vectors from each vertebral joint to the attachment locations when computing the stabilizing contribution of fascicle at a particular vertebral joint that is spanned by the fascicle (Figure 4.2).

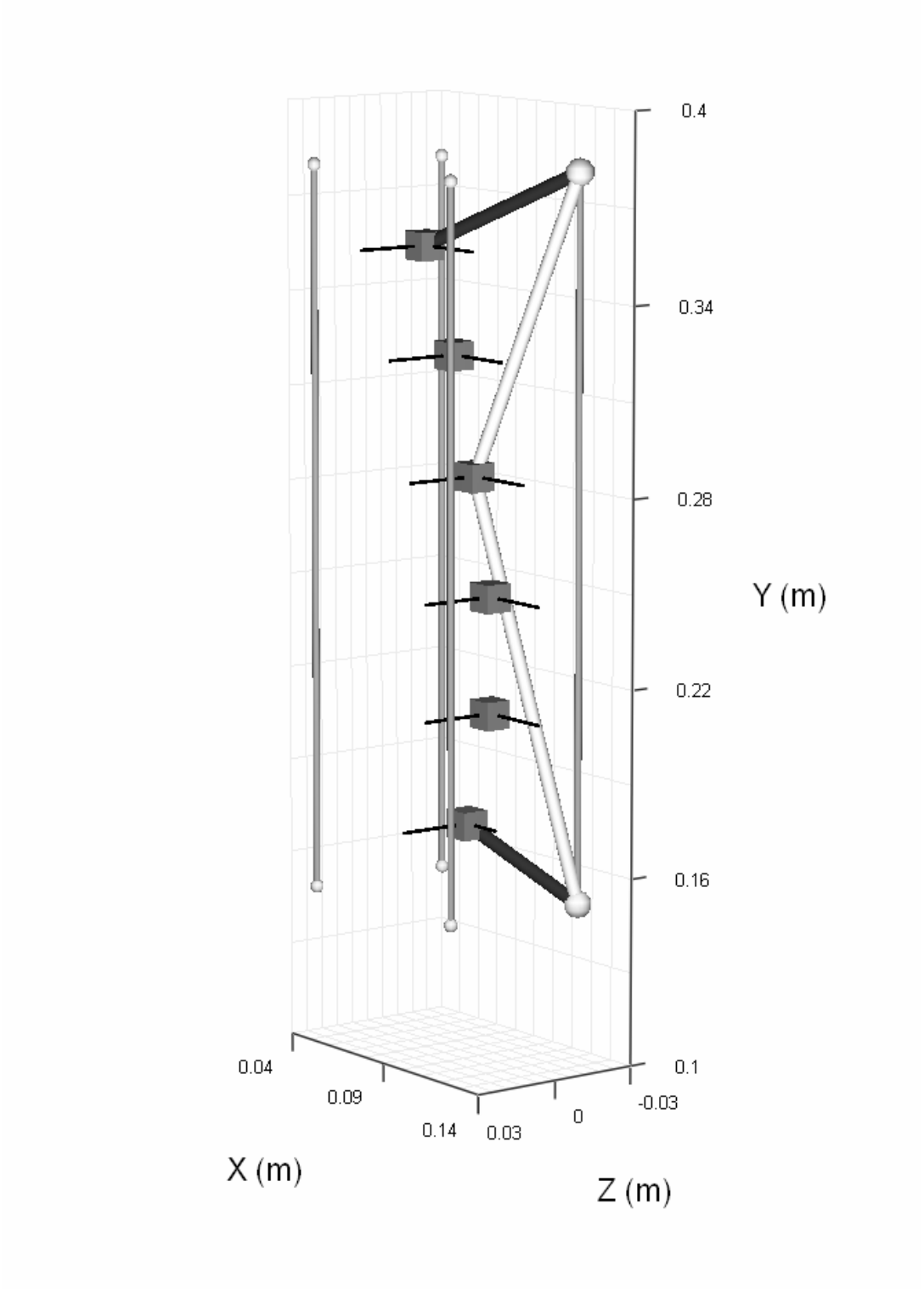

Figure 4.2 – An example of the difference in the set of vectors connecting vertebral joint centers and fascicle attachment locations considered by the method employed by Cholewicki & McGill (1996) and the method designed by Potvin & Brown (2005) in the case of a multisegmental fascicle without nodal points. Here the thick light grey bars indicate vectors used by Cholewicki and McGill (1996) and the thick dark grey bars indicate vectors used by Potvin and Brown (2005) for computation of the fascicle contribution at the L2-L3 vertebral joint.

The addition of nodal points to the multisegmental fascicles was performed to bring the two models back to better agreement on the vertebral joint and axis combination that was the least stiff. However, a second difference occurs in how the two models handle multisegmental fascicles with nodal points. The computational approach of Potvin & Brown (2005) only computed the stabilizing contribution of the segment that crossed the vertebral joint in question for a multisegmental fascicle with nodal points. On the other hand, Cholewicki & McGill (1996) consider the additive effects of the fascicle's other segments on stability at a given vertebral joint and axis.

4.2 – Comparison Between Eigenvector and Simplified Geometric Approach (Joint and Axis Analysis)

The likelihood of a discrepancy in the predicted location of likely buckling for the simulation with only axis fascicles was largest in lateral bend at the L4-L5 joint while the likelihood of a discrepancy was largest in flexion/extension at the L3-L4 joint for the simulation with the combined axis and quadrant fascicles (Figure 4.3).

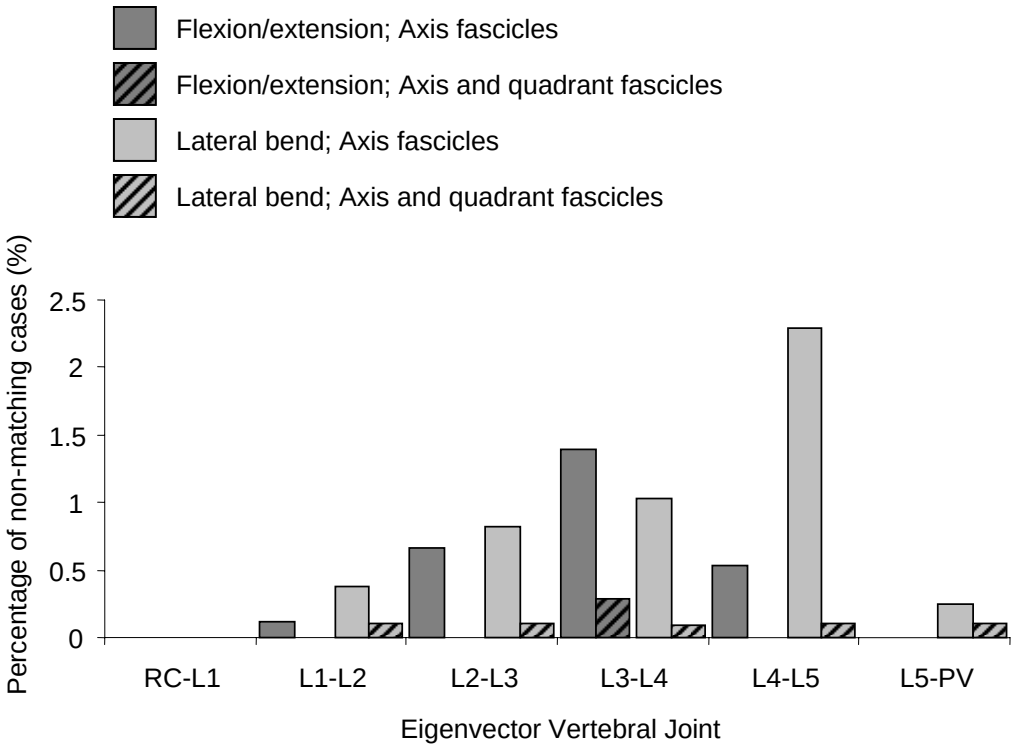

Figure 4.3 – The percentage of instances when the eigenvector predicted a given joint and axis as being the least stable and when the simplified geometric approach predicted a different joint and axis (100% = all instances when the eigenvector predicted a given joint and axis had discrepancies). Each bar in this figure represents a joint and axis combination with the two different patterns indicating different simulations and the different shades indicating different axes.

The addition of multisegmental fascicles that spanned the entire modeled lumbar spine without nodal points, to the existing set of axis and quadrant intersegmental fascicles generated the most likely discrepancies between the two models in flexion/extension at L3-L4, L4-L5, L5-Pelvis, and in lateral bend at L5-Pelvis (Figure 4.4a). The scales on the vertical axis for Figures 4.3 and 4.4 have different ranges to ensure that the data was visible. Adding nodal points to the multisegmental fascicles, and running the same instantiations as when the multisegmental fascicles did not have nodal points, reduced the likelihood of a discrepancy in flexion/extension at L3-L4, L4-L5, L5-Pelvis, and in lateral bend at L5-Pelvis. However, the addition of nodal points to the multisegmental fascicles increased the likelihood of discrepancies between the two models in lateral bend at L1-L2, L2-L3, L3-L4, and L4-L5 and in flexion/extension at L1-L2 (Figure 4.4b).

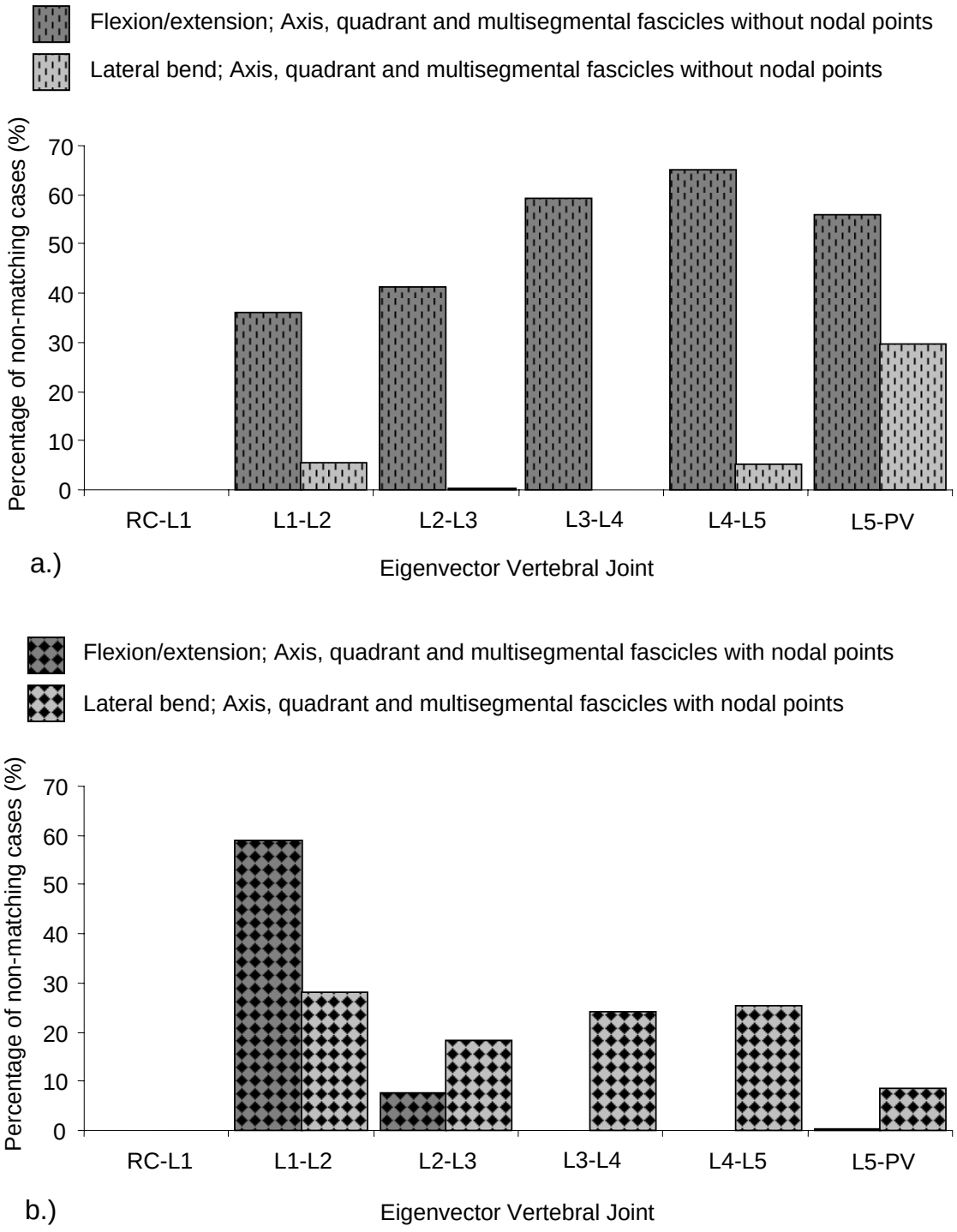

Figure 4.4 – The percentage of instances when the eigenvector predicted a given joint and axis as being the least stable and when the simplified geometric approach predicted a different joint and axis (100% = all instances when the eigenvector predicted a given joint and axis had discrepancies) for simulations with multisegmental muscles modeled without (a.) and with (b.) nodal points.

The simplified geometric approach tended to favour the lateral bend axis as being the least stable when the multisegmental fascicles were modeled without nodal points, and when a particular joint and axis combination was predicted by the eigenvector and a discrepancy occurred in the joint and axis combination predicted by the simplified geometric approach (Figure 4.5a). Conversely, the simplified geometric approach tended to favour the flexion/extension axis as being the least stable when a discrepancy occurred, and when modeling the multisegmental fascicles with nodal points (Figure 4.5b). When modeling the multisegmental fascicles without nodal points, the simplified geometric approach predicted flexion/extension at L3-L4 most frequently as the alternative joint and axis (Figure 4.5a). The simplified geometric approach predicted lateral bend at L4-L5 most frequently as the alternative joint and axis when using nodal points to model the multisegmental fascicles.

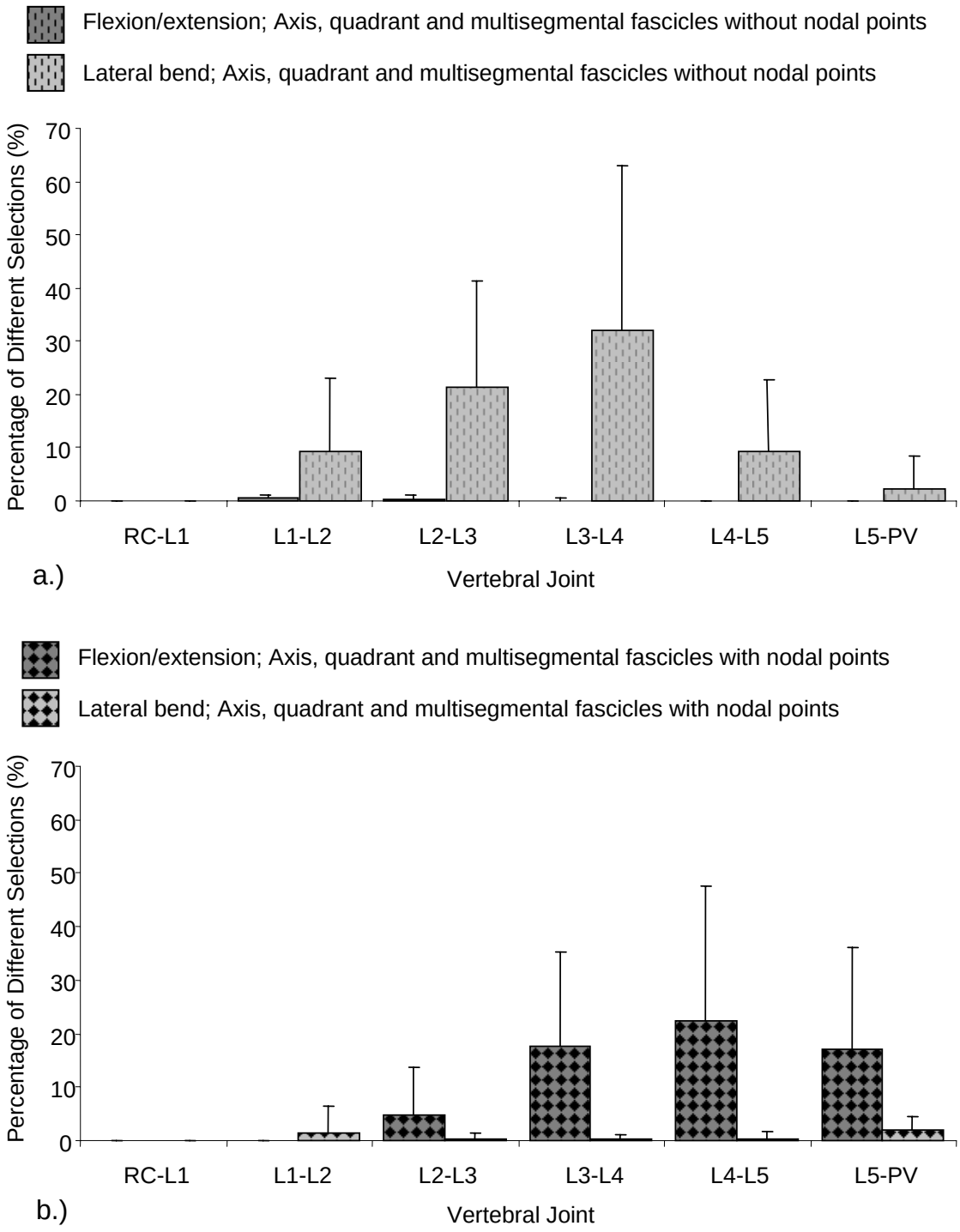

Figure 4.5 – The percentage of times that the simplified geometric method predicts each joint and axis when a discrepancy occurs between the joint and axis predicted by the eigenvector and the simplified geometric approach (100% = geometric method predicted this joint and axis in every case that there was a discrepancy) for simulations with multisegmental muscles modeled without (a.) and with (b.) nodal points.

4.3 – Cases Tested and Conditions for Achieving Stability

Stable and unstable configurations of muscle fascicle activity were tested in simulations 1.) – 3.) and 7.) (axis; axis and quadrant; axis, quadrant and multisegmental without nodal points; axis and multisegmental without nodal points) (Figure 4.6). The other simulations (4.) – 6.)) were omitted from this graph because simulation 4.) produced the same results as simulation 3.), and the results of simulations 5.) and 6.) were very similar to simulation 3.).

The percentage of stable configurations that were tested in each simulation, presented in Figure 4.6, was smallest for the simulation with axis and multisegmental muscle fascicles while the configurations with combined axis and quadrant muscle fascicles, and also multisegmental muscle fascicles tested many more mechanically stable cases (Figure 4.7). There was also a decrease in the number of mechanically stable configurations tested between the simulation with forty-eight muscle fascicles and the simulation with fifty-two muscle fascicles (Figure 4.7).

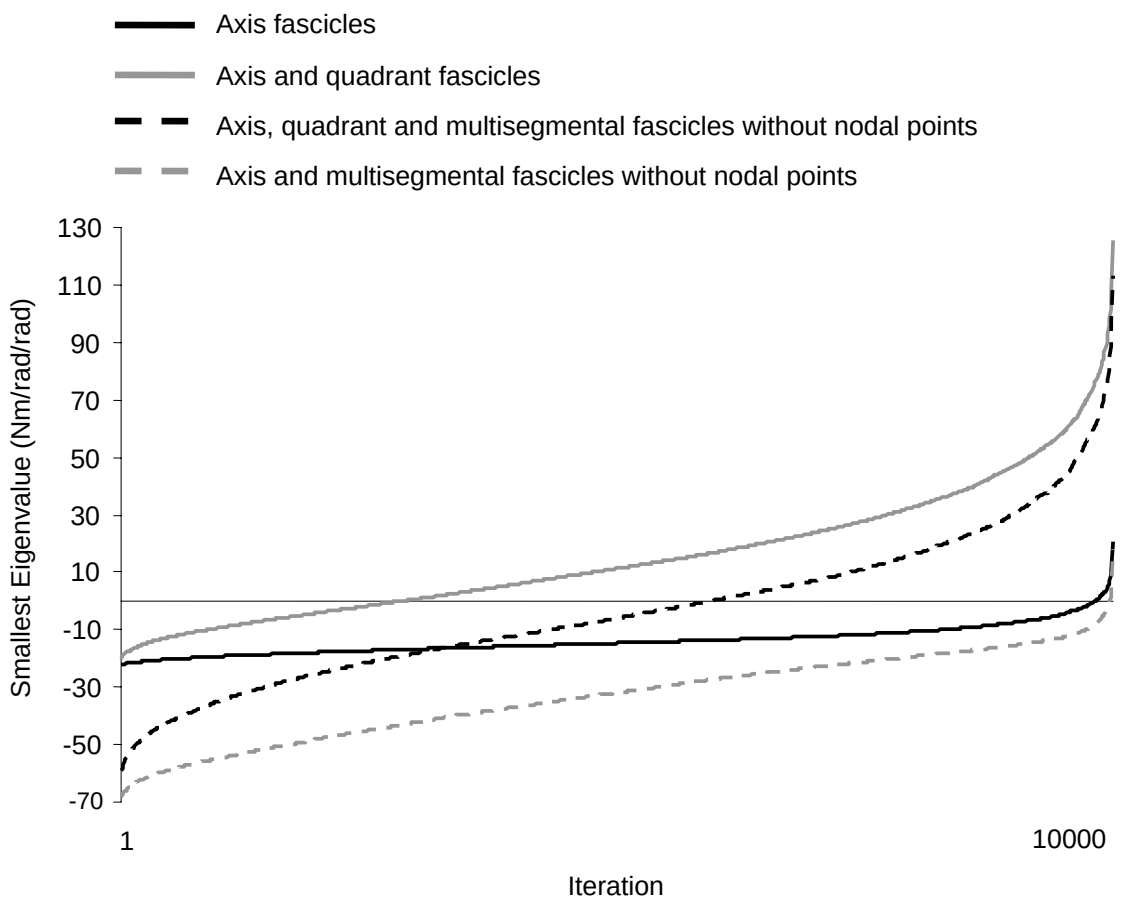

Figure 4.6 – The eigenvalues for each iteration for showing that both stable (smallest eigenvalue > 0) and unstable (smallest eigenvalue < 0) cases were tested. The legend above the graph indicates the set of fascicles that were used for the different simulations. The eigenvalues from each simulation were sorted in ascending order for this figure and is not indicative of the random order in which the different iterations were tested.

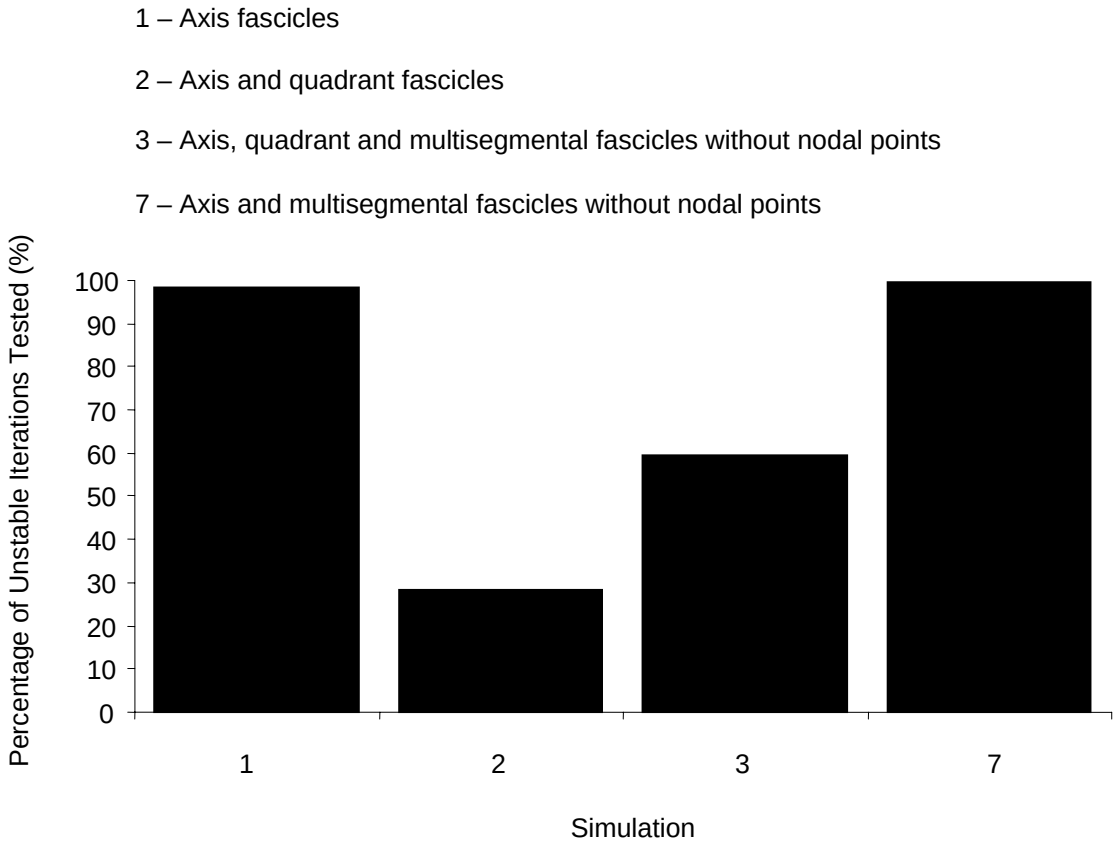

Figure 4.7 – The percentage (100% = 10000 iterations) of iterations that were deemed to be unstable by having a smallest eigenvalue that was less than zero. The legend above the graph indicates the set of fascicles that were used for the different simulations.

The axis fascicles were oriented such that each fascicle pair controlled the stiffness about a single axis at a single vertebral joint. Thus control over the stiffness for each axis (either flexion/extension or lateral bend) and at each vertebral joint was independent from every other axis and vertebral joint in the model. Analysis of the fascicle activation profiles for the simulation with only axis muscle fascicles shows that, on average, the fascicle activation, and subsequent force and stiffness, was spread over a smaller range in the stable cases than the unstable cases for both the flexion/extension and lateral bend degrees of freedom ($p < 0.0001$ for the fascicles controlling both the flexion/extension and lateral bend stiffness, Figure 4.8).

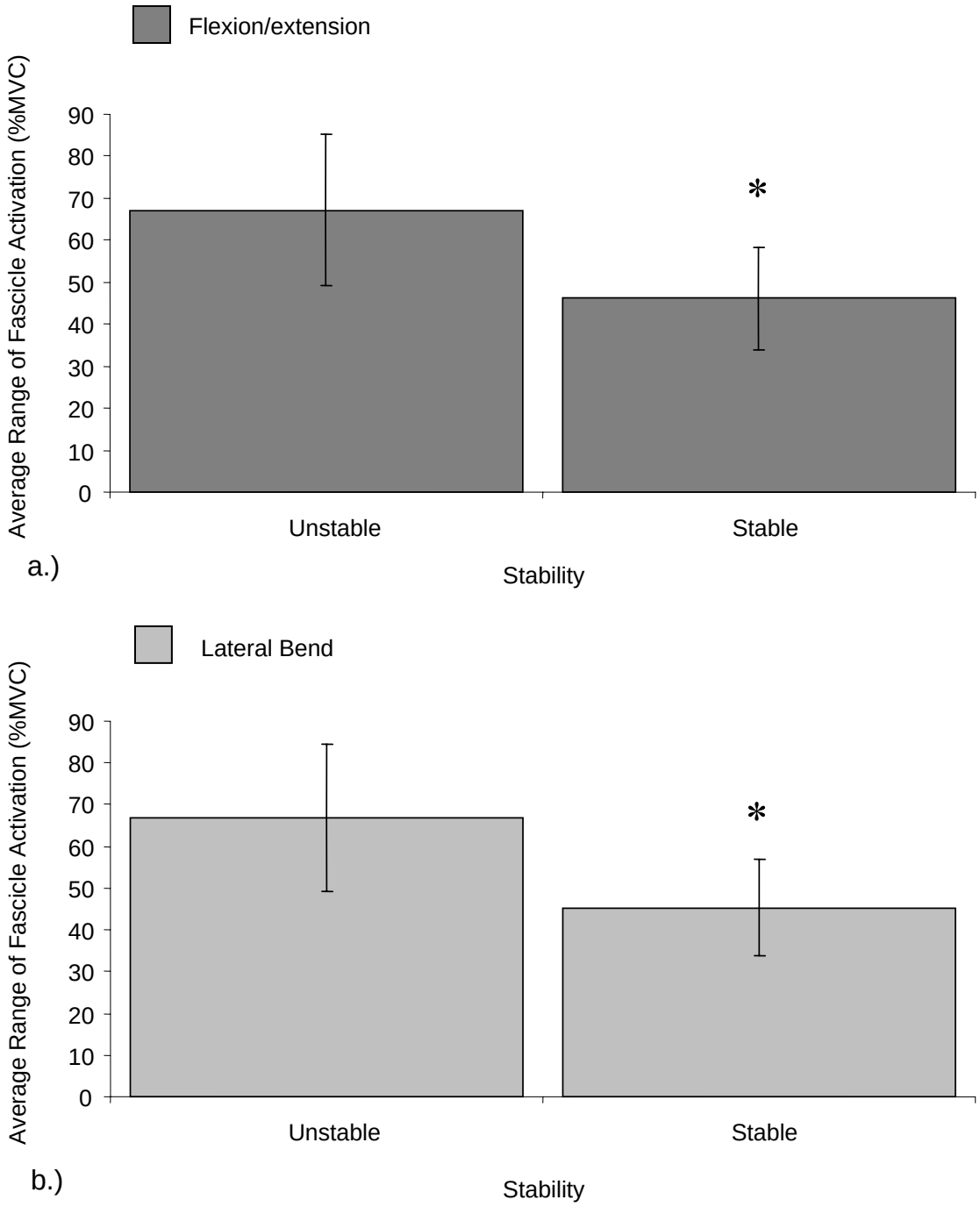

Figure 4.8 – Average range of fascicle activity across the flexion/extension (a.) and lateral bend (b.) axes for the simulation with axis fascicles. * indicates stable was significantly less than unstable ($p < 0.0001$).

V. DISCUSSION

5.1 – Feasibility of the eigenvector for locating instability

5.1.1 – Comparison of the Eigenvector to Vertebral Joint and Axis Rotational Stiffness Values

The first purpose of this investigation was to determine the feasibility of using the eigenvector for locating the least stiff vertebral joint and axis in a mathematical model of the human lumbar spine. The use of the eigenvector for locating the most likely joint and axis to buckle had been established in a model of the lumbar spine that consisted of only passive tissues which contributed to the vertebral joint rotational stiffness (Howarth & McGill, 2004). A second computational approach was employed to determine the contributions of individual muscle fascicles to vertebral joint and axis rotational stiffness. The rotational stiffness at each vertebral joint was used as a comparison to the outputs from the eigenvector determined using the traditional stability approach of analysing the second partial derivatives of the Hessian matrix. It was hypothesized that under an assumed form of the eigenvector, where each entry was associated with a particular vertebral joint and axis combination, the largest absolute value in the eigenvector would indicate the vertebral joint and axis with the least stiffness which is also the most likely joint and axis to become unstable.

The likelihood of the traditional stability approach and the simplified geometric approach for determining vertebral rotational stiffness with the inclusion of muscle fascicles was dependent on the conditions of the simulations. Specifically, the likelihood was dependent

on the number, and type (intersegmental or multisegmental) of fascicles that were modeled. In the simulations that consisted of only intersegmental fascicles (axis; axis and quadrant) the eigenvector and the simplified geometric approach predicted the same vertebral joint and axis as being the least stable in over 98% of the cases tested. The high degree of congruency can be attributed to the similarities between the computational procedures, and how the set of fascicles were constructed for these simulations. Likewise, the higher likelihood of a discrepancy in the least stable joint and axis between the two methods can be explained by differences in how the two models compute the contributions of multisegmental fascicles to stability at each vertebral joint that is spanned by the fascicle.

The simplified geometric approach for determining joint stiffness is an approximation of the terms on the main diagonal of the Hessian matrix. Thus, a discrepancy between the joint and axis selected as being the least stable between the two methods could occur if the off-diagonal terms in the Hessian matrix would influence the eigenvalue and subsequent eigenvector computation. The off-diagonal terms of the Hessian matrix represent the effects of one joint and axis on another. In the case of intersegmental fascicles, they have the ability to affect stability at a single joint, and will minimally affect off-diagonal terms in the Hessian matrix at very few entries if they are either rotated, or not aligned with the vertebral joint center (e.g. quadrant fascicles). If there is minimal activity in the off-diagonal terms of the Hessian matrix, then the set of eigenvalues will be very similar to the terms on the main diagonal of the Hessian matrix. Since the Hessian matrix is mathematically related to the complete set of eigenvalues, and their corresponding eigenvectors, there will be a value very close to 1 in the eigenvector entry that is associated with that particular Hessian matrix entry.

A simple example of a 3x3 symmetric matrix is shown below to illustrate the previous argument.

Example 1.

Consider the symmetric 3x3 matrix $\mathbf{M} = \begin{bmatrix} 34 & 0 & 3 \\ 0 & 24 & 1 \\ 3 & 1 & 9 \end{bmatrix}$. The corresponding eigenpairs (an eigenvalue with its eigenvector) for **M** are:

$8.5811, \quad (-0.117, -0.0643, 0.9911)$

$24.0626, \quad (-0.0189, 0.9979, 0.0625)$

$34.3563, \quad (-0.9930, -0.0114, -0.1179)$

Thus, assuming that the interpretation of the eigenvector (explained in section 3.7) is accurate, the simulations with only intersegmental fascicles produced a high likelihood of matching between the joint and axis that is most likely to be unstable primarily because of similarities between the computational approaches designed by Cholewicki & McGill (1996) and Potvin & Brown (2005) for this specific case.

Upon addition of the multisegmental fascicles to the model, the likelihood of a non-matching in the joint and axis determined to be the least stable increased. Although the addition of multisegmental fascicles will increase the off-diagonal contributions in the Hessian matrix because of their ability to affect the rotational degrees of freedom at many vertebral

joints, these contributions were not large enough to produce a significant change in the eigenvalues relative to the entries on the main diagonal of the Hessian matrix. Thus, a computational discrepancy in how the two methods determine the contributions of a multisegmental fascicle to stability is likely the cause of the increased likelihood of achieving a discrepancy between the traditional, and simplified geometric approaches. Specifically, the discrepancy was deemed to most likely occur in the set of vectors that each computational approach considered for computing a fascicle's contribution to stability at a joint that the fascicle spanned, but did not contain a vertebra to which the fascicle was attached. For example, there would be a discrepancy in the computational approaches when computing the contribution, at the L2-L3 vertebral joint, of a fascicle with attachments to the ribcage and pelvis (without intervening nodal points). The simplified geometric approach determines vectors from a vertebral joint center to the attachment points on the fascicle that spans the joint in order to determine the coordinates of the fascicle attachments relative to the current vertebral joint which is then used in the computation of the moment arm length along each of the three axes at a single vertebral joint. Conversely, approach employed by Cholewicki & McGill (1996) will determine a vector from each attachment location to each vertebra on the joint(s) to which the fascicle is attached. Again using the example of a multisegmental fascicle that spans from the ribcage to the pelvis (without intervening nodal points), the implementation of Cholewicki & McGill (1996) will determine one vector from the ribcage attachment to the Ribcage-L1 joint, and a second vector from the pelvic attachment to the Pelvis-L5 joint. These two vectors are then used in the computation of the fascicle's contribution to stability at each vertebral joint spanned by the fascicle.

Adding nodal points to the multisegmental fascicles was performed as an attempt to account for the aforementioned computational difference between the traditional stability approach, and the simplified geometric approach that approximated rotational stiffness for each vertebral joint and each axis. The addition of nodal points to create a multisegmental fascicle with a total of 6 segments creates the same set of vectors from the vertebral joint center to the fascicle attachment and nodal locations for the traditional stability approach and the simplified geometric approach for determining vertebral joint stiffness. Computationally, this should have created a situation that was similar to the simulations where only intersegmental fascicles were modeled. Thus we would expect to see similar results between the simulation with multisegmental fascicles with nodal points, and the simulations that only used intersegmental fascicles.

Although this adjustment improved the likelihood that the two computational approaches would determine the same vertebral joint and axis as being the most likely to buckle, adding nodal points to the multisegmental fascicles did not achieve similar levels of agreement that were observed for the cases with only intersegmental fascicles. This can be attributed to another difference in how the two computational methods assess the contributions of a multisegmental fascicle to each joint and axis that it spans. The simplified geometrical approach to determine vertebral joint stiffness only considers the effect of the single segment of a multisegmental fascicle with nodal points that crosses each vertebral joint on the vertebral joint's stiffness. Comparatively, the traditional stability approach will consider the effect of the single segment of a multisegmental fascicle with nodal points that crosses a vertebral joint in conjunction with the additive effects of the fascicle's other segments on the stability of that

vertebral joint.

5.1.2 – The Assumption of a Vertical Column and its Influence on the Eigenvector's Ability to Predict the Location of Likely Buckling

Traditionally, the eigenvector is used to determine the buckled configuration of a vertical column under an applied compressive load (Farshad, 1994). Previous work by Crisco and Panjabi (1992) has used the eigenvector to determine the buckled configuration of a mathematical model of the passive lumbar spine (no muscles were included) in the frontal plane. Their analysis was restricted to the frontal plane because the curvature of the lumbar spine would violate the assumption of a vertical and straight column that is inherent in structural stability analysis. However, this investigation showed that the assumption of a straight and vertical column is likely not violated by the mathematical construction of the local coordinate systems at each vertebral joint. In the model described by Cholewicki & McGill (1996), the local coordinate system at each vertebral joint is aligned with the global coordinate system which is consistent with the ISB defined convention for the spine (Wu et al, 2002). Hence, when the vertebral joint centers were aligned to generate a straight column, the outputs from the comparison between the two methods were identical because the inputs to the computations were identical. Based on the reasoning of Crisco and Panjabi (1992), and the evidence of the current investigation with regards to the assumption that the column must be straight, the eigenvector appears to be a suitable means for determining the least stable vertebral joint and axis.

5.1.3 – Biases in Discrepancies

The likelihood of a discrepancy occurring between the eigenvector and the simplified geometrical approach for determining the location of the least stable vertebral joint and axis varied depending on the vertebral joint and the set of fascicles used in the simulation. This was particularly evident in the simulations that included multisegmental fascicles. Unlike the intersegmental fascicles, the multisegmental fascicles could not be created in a manner that completely balanced the moments at every vertebral joint. In particular, the addition of multisegmental fascicles without nodal points creates more unbalanced moments at the vertebral joints near the apex of the lumbar curvature (L3-L4, and L4-L5) and at the flexion/extension axis of these joints. The difference in the likelihood of a discrepancy at each combination of vertebral joints and axes indicates a relative degree of certainty that one can have if using the eigenvector for locating the least stable vertebral joint and axis. Changing the way in which the multisegmental fascicles were modeled (i.e. adding nodal points) changed the likelihood of a discrepancy at each joint and axis combination. This suggests that the way in which fascicles are modeled should be considered when evaluating the effectiveness of the eigenvector for locating the least stable vertebral joint and axis.

5.1.4 – Limitations

The methods used for identifying the feasibility of the eigenvector for are mathematical approximations of reality. Thus, even if it was certain that the eigenvector was able to determine the least stable vertebral joint and axis, any conclusion with regards to the stability

of the lumbar spine must consider that the mathematical approximation may not directly reflect reality. This investigation considered a very specific set of fascicles that were designed to provide simple manipulation over the vertebral joint stiffness about either the flexion/entension, lateral bend, or a combination of both axes. Although the orientations of the fascicles were contrived with a specific purpose, they were oriented in a manner that could also provide biological validity. Consequently, it was difficult to create a set of fascicles that independently controlled the axial twist degree of freedom at each vertebral level and maintaining biological validity. Thus, the passive contributions to stability in the mode of axial rotation at each vertebral joint were increased to disallow this rotational degree of freedom from being selected as the least stable via its lack of stiffness provided by active fascicles. Increasing the passive tissue properties in the mode of axial rotation did not affect the stability of the other vertebral joints and axes. Thus, it was deemed feasible to eliminate the mode of axial rotation from the analysis.

The contribution of bodyweight to stability was added to Ribcage-L1 joint, and mathematically increased the stiffness at this joint. The increase in stiffness was large enough that neither the eigenvector, nor the simplified geometrical approach predicted either of the axes (flexion/extension or lateral bend) as being the least stable for any iteration in any of the simulations. It would be less realistic to consider the stability of the spine without the inclusion of a mass above the spine. Thus, bodyweight was included in all simulations to increase the biological validity at the expense of being able to test the feasibility of the eigenvector for locating the Ribcage-L1 joint as being the least stable.

The feasibility of the eigenvector for locating instability remains largely unknown. Although other groups have used the eigenvector for determining buckled configurations (Crisco & Panjabi, 1992; Gardner-Morse et al, 1995), the relationship of the eigenvector's individual entries to the buckled configuration and subsequent least stable location has never been presented. This study attempted to validate a form of the eigenvector that was proposed in an investigation of the stability of the passive lumbar spine (Howarth & McGill, 2005). The method used here to validate the form of the eigenvector was a derivative of the traditional stability approach described by Cholewicki & McGill (1996). Thus it can be argued that the validity of the eigenvector for determining the least stable location that was established in this investigation is merely a consequence of congruity between the two computational approaches. However, it has been demonstrated that while the two approaches are based on the same theory, their computational differences that are discussed above reduce the likelihood that agreement on the least stable vertebral joint and axis is an artefact of their common roots.

5.2 – Recruitment of Fascicle Activation for Achieving Stability

The results discussed in the following sections are based on outputs from the traditional stability model (Cholewicki & McGill, 1996). Thus, stability is achieved when the smallest eigenvalue of the Hessian matrix is greater than zero, and instability occurs when the smallest eigenvalue of the Hessian matrix is less than zero.

5.2.1 – Intersegmental Versus Multisegmental Fascicles for Achieving Stability

Bergmark's (1989) original work on mechanical stability computation for the lumbar spine defined muscle fascicles as being global or local fascicles. The intent here was that global fascicles could produce stiffness and stability over a larger range of vertebral joints than the local muscles. Panjabi (1989) extended the discrepancy between local and global fascicles by indicating that the global fascicles were designed for moment generation, while the local fascicles were used to provide stability. This investigation showed that adding multisegmental fascicles to a set of intersegmental fascicles reduced the ability of the spine to generate stability. This suggests that mutlisegmental fascicles, although efficient for providing stability to many vertebral joints, may lead to a higher likelihood of instability.

For this investigation, multisegmental fascicles were designed to vertically span the entire modeled lumbar spine (see Figure 3.5). The curvature of the spine limits the ability to activate these fascicles in a manner that will achieve moment equilibrium at every vertebral joint. Moment equilibrium is a principal assumption in mechanical stability analysis, and is achieved in the complete model of the lumbar spine (Cholewicki & McGill, 1996) by using an EMG guided optimization routine for balancing muscle moments (Cholewicki & McGill, 1995). However, the moments generated by the multisegmental fascicles at each vertebral joint were not balanced which subsequently led to a higher number of unstable cases tested when multisegmental fascicles were added to the model. However, the beneficial effects of multisegmental fascicles for simultaneously providing stability to many vertebral levels should not be ignored. The results from this investigation suggest that activating multisegmental

fascicles will increase the rotational stiffness of the spine, but will also require proper activation of other fascicles in order to achieve balancing of the moments at each vertebral joint. Thus, the paradox that arises when activating multisegmental fascicles is that they have the ability to influence stability at many different vertebral levels, but if not activated in a proper manner, the multisegmental fascicles can reduce the stability of the lumbar spine. This lends support to the idea put forth by McGill (2003), and Kavcic and colleagues (2004) that stability is achieved through the coordinated activation of many muscles surrounding the lumbar spine, and not by activating a single group of muscles. Clinically this implies that focusing on the activation of a single muscle for achieving stability may be a faulty approach because inappropriate activation of a

The number of stable cases tested increased when the quadrant fascicles were added to the axis fascicles. Quadrant fascicles were designed to simultaneously influence the rotational stiffness about the flexion/extension and lateral bend axes at a single vertebral joint while the axis fascicles were designed to influence a the rotational stiffness about a single axis at a single vertebral joint. Control over the balance of the moments generated by the fascicles was achieved since both sets (axis and quadrant) of fascicles only spanned a single vertebral joint. Thus, the large increase in the number of stable cases, as determined by the smallest eigenvalue, tested in the simulation with the combined set of axis and quadrant fascicles was a result of increased vertebral joint rotational stiffness provided by the additional intersegmental fascicles. Clinically, this implies that intersegmental fascicles are efficient for controlling the stability of an individual vertebral level, and could also be beneficial for creating a balanced moment at each vertebral level in the presence of a multisegmental fascicle. The increased

number of stable cases with the addition of more intersegmental fascicles and the subsequent decrease in the number of stable cases upon the introduction of multisegmental fascicles also provides support for Panjabi's (1989) concept that the larger, global muscles are used for moment generation while the smaller local muscles are important for providing stability.

5.2.2 – Clinical Relevance of Coordinated Activation of Fascicle Activity for Achieving Stability

Debate currently exists over how to achieve stability within the lumbar spine. One method is to focus on activating specific muscles that have been termed "stabilizers" while another method focuses on activating a collection of muscles in order to achieve a stable spine. The second purpose of this investigation was designed to investigate the conditions that mathematically contribute to creating stability.

This investigation has shown that cases where the lumbar spine was deemed to be mechanically stable was characterised by a smaller range of fascicle activation across all vertebral joints and axes in a simulation where each fascicle controlled the stiffness of a single axis at a single vertebral joint. The range of fascicle activity was used to quantify the coordination of the fascicle activity since it has been hypothesized that proper coordination of muscle activity can achieve stability (McGill et al, 2003). The rationale for using the range of fascicle activity was that a smaller range would indicate that the activity of all fascicles would be better coordinated and thus would increase the stability of the lumbar spine. The statistical analyses of the average range of fascicle activity indicate that there is very strong evidence to

support the claim that stability is governed by having a better balance between the activities of all fascicles. The requirement for a reduced range of fascicle activity that yields a more balanced pattern of fascicle activation contradicts the idea that there is a rank order of muscles for improving stability of the lumbar spine. In particular, the Queensland group emphasize retraining of the multifidus muscle for improving stability, and then incorporating the multifidus activity into daily activities (MacDonald et al, 2006). This approach is based on the observation that patients diagnosed with lumbar instability have a reduced ability to properly recruit the multifidus muscle during daily tasks. This group also emphasizes activation of the transversus abdominis muscle for improving stability of the lumbar spine (Hodges et al, 1997). Evidently, their approach for achieving stability is strongly focused on activating specific muscles. Conversely, the evidence from this investigation is supported by the fact that the relative importance of the muscles for providing stability is dependent on the position and external loading conditions (Cholewicki & VanVliet, 2002; Kavcic et al, 2004). Moreover, this evidence supports the claim that stability is achieved through well-coordinated patterns of muscle activation (McGill et al, 2003).

5.2.3 – Limitations

The clinically relevant finding of this section is based on the stability outputs from a lumbar spine that consists of an artificial set of muscle fascicles. Each fascicle was given an identical PCSA, no tendon, and all intersegmental fascicles were given identical lengths while all multisegmental fascicles were also given identical lengths. This was done in order to control the effects of PCSA, non-linear tendon force-stiffness properties and fascicle length on

the stability and stiffness outputs for the primary purpose of this investigation. Furthermore, the orientation of each fascicle was kept vertical. Modeling the fascicles with an oblique line of action would be beneficial for mimicking the effects that muscles such as internal and external oblique have on stability.

VI. CONCLUSIONS AND CLINICAL IMPLICATIONS

This study attempted to determine the feasibility of using the eigenvector, derived from a mathematical approach that calculates the stability of the lumbar spine, for locating the least stable vertebral joint and axis. Traditionally, the eigenvector is used as an indicator of the buckled configuration of structures. For this analysis, a proposed form of the eigenvector was compared to the outputs of a computational method that approximated individual vertebral joint stiffness for each rotational axis. However, due to congruency between the two methods, it is still unclear whether or not the eigenvector can successfully locate the least stable joint and axis in the presence of a set of active muscle fascicles. Nonetheless, evidence exists for using the eigenvector for determining the buckled configuration of the spine, and for determining the location of least stiffness in a passive system. The decision from this investigation is that the proposed form of the eigenvector provides an initial approximation of the least stable joint and axis, but it should not be used as the definitive indicator of the least stable joint and axis.

The secondary purpose of this work was to determine the conditions for generating stability. The results presented here support the hypothesis that stability is achieved through coordinated activation of a group of muscles instead of focusing on the activation of a single muscle. This information is relevant for clinicians prescribing motor pattern training for improving the unstable lumbar spine. It was also determined that the ability of multisegmental muscles (e.g. rectus abdominis) to provide stability is dependent of the fine control of other muscles at each vertebral joint.

VII. FUTURE DIRECTIONS

The current investigation did not consider what happens to stability and the eigenvector when the lumbar spine is rotated away from its initial geometrical configuration. Furthermore, the effects of an external load on the eigenvector should also be investigated. However, to test these conditions, it would be advisable to create a physical model with the identical musculature and passive properties to the computer generated model of the lumbar spine used for this investigation. This would allow for direct measurement of the resulting configuration from the applied compressive load and evaluation of the least stable vertebral joint and axis from the physical model. The parameters of fascicle force, stiffness and applied compressive load could be entered into the computer generated model to verify that the eigenvector predicted the same least stable location that was measured from the physical model.

VIII. APPENDICES

Appendix A.

The contents of this appendix were taken from Cholewicki and McGill (1996) and is a mathematical derivation of the terms, and the subsequent partial derivatives of the potential energy function that is used in the mechanical analysis of lumbar spine stability.

Appendix B: Stability analysis

At any given frame, the potential of the spine system (V) is expressed as the sum of the elastic energy stored in the linear springs (U_L) (muscles and tendons), elastic energy stored in the torsional springs (U_T) (lumped intervertebral joint discs, ligaments and other passive tissues) minus the work performed on the external load (W):

$$V = U_L + U_T - W \tag{B1}$$

Partial derivatives of the potential V were calculated separately for each component taking the Euler angles α_i (3 rotation angles × 6 joints = 18 df) as the generalized coordinates:

$$\frac{\partial V}{\partial \alpha_i} = \frac{\partial U_L}{\partial \alpha_i} + \frac{\partial U_T}{\partial \alpha_i} - \frac{\partial W}{\partial \alpha_i}$$

$$\frac{\partial^2 V}{\partial \alpha_i \partial \alpha_j} = \frac{\partial^2 U_L}{\partial \alpha_i \partial \alpha_j} + \frac{\partial^2 U_T}{\partial \alpha_i \partial \alpha_j} - \frac{\partial^2 W}{\partial \alpha_i \partial \alpha_j} \tag{B2}$$

The energy stored in linear springs (U_L) can be expressed as follows:

$$U_L = \sum_{m=1}^{90} F_m (l_{p_m} - l_{o_m}) + \frac{1}{2} K_m (l_{p_m} - l_{o_m})^2 \tag{B3}$$

where
F_m = instantaneous muscle force (N),
K_m = instantaneous muscle stiffness (N/m),
l_{om}, l_{pm} = original ('frozen' in a given frame) and perturbed muscle lengths (m), and

$$\frac{\partial U_L}{\partial \alpha_i} = \sum_{m=1}^{90} [F_m + K_m (l_{p_m} - l_{o_m})] \frac{\partial l_{p_m}}{\partial \alpha_i}$$

$$\frac{\partial^2 U_L}{\partial \alpha_i \partial \alpha_j} = \sum_{m=1}^{90} K_m \frac{\partial l_{p_m}}{\partial \alpha_j} \frac{\partial l_{p_m}}{\partial \alpha_i} + [F_m + K_m (l_{p_m} - l_{o_m})] \frac{\partial^2 l_{p_m}}{\partial \alpha_j \partial \alpha_i} \tag{B4}$$

Since the partial derivatives are evaluated at the unperturbed point of equilibrium, $l_{pm} - l_{om} = 0$ and the Equations (B4) reduce to the following:

$$\frac{\partial U_L}{\partial \alpha_i} = \sum_{m=1}^{90} F_m \frac{\partial l_{p_m}}{\partial \alpha_i}$$

$$\frac{\partial^2 U_L}{\partial \alpha_i \partial \alpha_j} = \sum_{m=1}^{90} K_m \frac{\partial l_{p_m}}{\partial \alpha_j} \frac{\partial l_{p_m}}{\partial \alpha_i} + F_m \frac{\partial^2 l_{p_m}}{\partial \alpha_j \partial \alpha_i} \tag{B5}$$

If the muscle length is represented with a sum of n sections (when the muscle passes through the nodal point), its potential energy derivatives consist of a sum of its sections with some additional terms. Thus, if $l_{om} = l_{om1} + l_{om2} + .. + l_{omn}$ and $l_{pm} = l_{pm1} + l_{pm2} + .. + l_{pmn}$ then

$$\frac{\partial U_{L_m}}{\partial \alpha_i} = \sum_{n=1}^{\text{nodes}+1} \frac{\partial U_{L_{mn}}}{\partial \alpha_i}$$

$$\frac{\partial^2 U_{L_m}}{\partial \alpha_i \partial \alpha_j} = \sum_{n=1}^{\text{nodes}+1} \frac{\partial^2 U_{L_{mn}}}{\partial \alpha_i \partial \alpha_j} + K_m \sum_{r \neq s}^{\text{nodes}+1} \frac{\partial l_{p_{mr}}}{\partial \alpha_j} \frac{\partial l_{p_{ms}}}{\partial \alpha_i} \tag{B6}$$

Since the length of a given muscle l_p (dropping the muscle subscript 'm' at this point) is given by the vector sum of the length components in the X, Y and Z axes direction,

$$l_p = (l_{px}^2 + l_{py}^2 + l_{pz}^2)^{1/2} \tag{B7}$$

then

$$\frac{\partial l_p}{\partial \alpha_i} = (l_{px}^2 + l_{py}^2 + l_{pz}^2)^{-1/2}\left(l_{px}\frac{\partial l_{px}}{\partial \alpha_i} + l_{py}\frac{\partial l_{py}}{\partial \alpha_i} + l_{pz}\frac{\partial l_{pz}}{\partial \alpha_i}\right) \tag{B8}$$

and

$$\begin{aligned}\frac{\partial^2 l_p}{\partial \alpha_i \partial \alpha_j} = &-(l_{px}^2 + l_{py}^2 + l_{pz}^2)^{-3/2}\left(l_{px}\frac{\partial l_{px}}{\partial \alpha_i} + l_{py}\frac{\partial l_{py}}{\partial \alpha_i} + l_{pz}\frac{\partial l_{pz}}{\partial \alpha_i}\right)\\ &\left(l_{px}\frac{\partial l_{px}}{\alpha_j} + l_{py}\frac{\partial l_{py}}{\alpha_j} + l_{pz}\frac{\partial l_{pz}}{\alpha_j}\right) + (l_{px}^2 + l_{py}^2 + l_{pz}^2)^{-1/2}\\ &\left(\frac{\partial l_{px}}{\partial \alpha_j}\frac{\partial l_{px}}{\partial \alpha_i} + l_{px}\frac{\partial^2 l_{px}}{\partial \alpha_i \partial \alpha_j} + \frac{\partial l_{py}}{\partial \alpha_j}\frac{\partial l_{py}}{\partial \alpha_i}\right.\\ &\left. + l_{py}\frac{\partial^2 l_{py}}{\partial \alpha_i \partial \alpha_j} + \frac{\partial l_{pz}}{\partial \alpha_j}\frac{\partial l_{pz}}{\partial \alpha_i} + l_{pz}\frac{\partial^2 l_{pz}}{\partial \alpha_i \partial \alpha_j}\right)\end{aligned} \tag{B9}$$

Substituting (B6), (B7) and (B8) into (B4) yields

$$\frac{\partial U_{L_m}}{\partial \alpha_i} = F_m(l_{px}^2 + l_{py}^2 + l_{pz}^2)^{1/2}\left(l_{px}\frac{\partial l_{px}}{\partial \alpha_i} + l_{py}\frac{\partial l_{py}}{\partial \alpha_i} + l_{pz}\frac{\partial l_{pz}}{\partial \alpha_i}\right) \tag{B10}$$

and

$$\begin{aligned}\frac{\partial^2 U_{L_m}}{\partial \alpha_i \partial \alpha_j} = &(K_m l_p^{-2} - F_m l_p^{-3})\left[\left(l_{px}\frac{\partial l_{px}}{\partial \alpha_i} + l_{py}\frac{\partial l_{py}}{\partial \alpha_i} + l_{pz}\frac{\partial l_{pz}}{\partial \alpha_i}\right)\right.\\ &\left.\left(l_{px}\frac{\partial l_{px}}{\alpha_j} + l_{py}\frac{\partial l_{py}}{\alpha_j} + l_{pz}\frac{\partial l_{pz}}{\alpha_j}\right)\right]\\ &+ F_m l_p^{-1}\left(\frac{\partial l_{px}}{\partial \alpha_j}\frac{\partial l_{px}}{\partial \alpha_i} + l_{px}\frac{\partial^2 l_{px}}{\partial \alpha_i \partial \alpha_j} + \frac{\partial l_{py}}{\partial \alpha_j}\frac{\partial l_{py}}{\partial \alpha_i}\right.\\ &\left. + l_{py}\frac{\partial^2 l_{py}}{\partial \alpha_i \partial \alpha_j} + \frac{\partial l_{pz}}{\partial \alpha_j}\frac{\partial l_{pz}}{\partial \alpha_i} + l_{pz}\frac{\partial^2 l_{pz}}{\partial \alpha_i \partial \alpha_j}\right)\end{aligned} \tag{B11}$$

It remains to evaluate partial derivatives of muscle length components l_{px}, l_{py}, l_{pz} in relation to all 18 rotation angles α_i. If the muscle originates on a skeletal segment 'w' and inserts onto the segment 'u' (Figure 3), then its length vector

$$\begin{aligned}\begin{bmatrix} l_{px} \\ l_{py} \\ l_{pz} \end{bmatrix} = &[\lambda_u]\begin{bmatrix} X_u - OX_u \\ Y_u - OY_u \\ Z_u - OZ_u \end{bmatrix} - [\lambda_w]\begin{bmatrix} X_w - OX_w \\ Y_w - OY_w \\ Z_w - OZ_w \end{bmatrix}\\ &+ [\lambda_{u+1}][L_{u+1}] + \cdots + [\lambda_w][L_w]\\ &u,\ w = 0, \ldots 6,\ w > u\end{aligned} \tag{B12}$$

where
λ is a rotation matrix,
L is the vector of vertebral segment lengths taken between the adjacent joints,
X, Y, Z are coordinates of the muscle attachment points in the reference posture,
OX, OY, OZ are coordinates of the rotation centre (a joint) of a given segment.
Partial derivatives of the elements of rotation matrices were easily programmed on a computer by inserting the appropriate derivatives of the trigonometric functions.

To obtain the elastic energy, which is stored in all of the torsional springs, we need to integrate the Equation (1) with respect to the relative joint angles and sum it over the 6 joints:

$$\begin{aligned}U_{Tx} = &\sum_{j=0}^{5}\int M_{xj}d(\phi_j - \phi_{j+1}) = \sum_{j=0}^{5}\frac{a_{xj}}{b_{xj}}[e^{b_{xj}(\phi_j - \phi_{j+1})}\\ &- b_{xj}(\phi_j - \phi_{j+1})] + K(\psi_j - \psi_{j+1})(\phi_j - \phi_{j+1})\\ U_{Ty} = &\sum_{j=0}^{5}\int M_{yj}d(\psi_j - \psi_{j+1}) = \sum_{j=0}^{5}\frac{a_{yj}}{b_{yj}}[e^{b_{yj}(\psi_j - \psi_{j+1})}\\ &- b_{yj}(\psi_j - \psi_{j+1})] + K(\phi_j - \phi_{j+1})(\psi_j - \psi_{j+1})\\ U_{Tz} = &\sum_{j=0}^{5}\int M_{zj}d(\theta_j - \theta_{j+1}) = \sum_{j=0}^{5}\frac{a_{zj}}{b_{zj}}[e^{b_{zj}(\theta_j - \theta_{j+1})}\\ &- b_{zj}(\theta_j - \theta_{j+1})]\end{aligned} \tag{B13}$$

The first partial derivatives of U_T will have two terms belonging to the two adjacent intervertebral joints:

$$\begin{aligned}\frac{\partial U_T}{\partial \phi_j} = &a_{xj}[e^{b_{xj}(\phi_j - \phi_{j+1})} - 1] + K(\psi_j - \psi_{j+1})\\ &- a_{x(j-1)}[e^{b_{x(j-1)}(\phi_{j-1} - \phi_j)} - 1] - K(\psi_{j-1} - \psi_j)\\ \frac{\partial U_T}{\partial \psi_j} = &a_{yj}[e^{b_{yj}(\psi_j - \psi_{j+1})} - 1] + K(\phi_j - \phi_{j+1})\\ &- a_{y(j-1)}[e^{b_{y(j-1)}(\psi_{j-1} - \psi_j)} - 1] - K(\phi_{j-1} - \phi_j)\\ \frac{\partial U_T}{\partial \theta_j} = &a_{zj}[e^{b_{zj}(\theta_j - \theta_{j+1})} - 1] + a_{z(j-1)}[e^{b_{z(j-1)}(\theta_{j-1} - \theta_j)} - 1]\end{aligned} \tag{B14}$$

For the negative angles, coefficients 'a' and 'b' will appear with a minus sign and the appropriate constants will be inserted in the case of flexion. Now, there are six second partial derivatives of the U_T possible for the general case:

$$\begin{aligned}\frac{\partial^2 U_T}{\partial \phi_j \partial \phi_{j-1}} &= -a_{x(j-1)}b_{x(j-1)}e^{b_{x(j-1)}(\phi_{j-1} - \phi_j)}\\ \frac{\partial^2 U_T}{\partial \phi_j^2} &= a_{xj}b_{xj}e^{b_{xj}(\phi_j - \phi_{j+1})} + a_{x(j-1)}b_{x(j-1)}e^{b_{x(j-1)}(\phi_{j-1} - \phi_j)}\\ \frac{\partial U_T}{\partial \phi_j \partial \phi_{j+1}} &= -a_{xj}b_{xj}e^{b_{xj}(\phi_j - \phi_{j+1})}\\ \frac{\partial^2 U_T}{\partial \phi_j \partial \psi_{j-1}} &= \frac{\partial^2 U_T}{\partial \phi_j \partial \psi_{j+1}} = -K\\ \frac{\partial^2 U_T}{\partial \phi_j \partial \psi_j} &= 2K\end{aligned} \tag{B15}$$

An identical equation format results if the U_T formulation of twist is differentiated twice. Flexion/extension has the same general format as (B15), except $K \approx 0$ in this case.

The external work W performed by the load P is a dot product of the force and displacement vectors:

$$W = \vec{P} \cdot \Delta\vec{h} = P_x(h_{px} - h_{ox}) + P_y(h_{py} - h_{oy}) + P_z(h_{pz} - h_{oz}) \tag{B16}$$

where h_p and h_o are the perturbed and the original points of force application. Thus,

$$\frac{\partial W}{\partial \alpha_i} = F_x \frac{\partial h_{px}}{\partial \alpha_i} + F_y \frac{\partial h_{py}}{\partial \alpha_i} + F_z \frac{\partial h_{pz}}{\partial \alpha_i}$$

$$\frac{\partial^2 W}{\partial \alpha_i \partial \alpha_j} = F_x \frac{\partial^2 h_{px}}{\partial \alpha_i \partial \alpha_j} + F_y \frac{\partial^2 h_{py}}{\partial \alpha_i \partial \alpha_j} + F_z \frac{\partial^2 h_{pz}}{\partial \alpha_i \partial \alpha_j} \tag{B17}$$

Since the load P is always applied to the ribcage,

$$\begin{bmatrix} h_{px} \\ h_{py} \\ h_{pz} \end{bmatrix} = [\lambda_0] \begin{bmatrix} X_{h0} - OX_0 \\ Y_{h0} - OY_0 \\ Z_{h0} - OZ_0 \end{bmatrix} + [\lambda_1][L_1] + \cdots + [\lambda_6][L_6] \tag{B18}$$

The derivatives of the rotation matrix [λ] are the same in Equation (B12). Because the global axes system is imbedded into the pelvis, the last term in Equation (B18) vanishes upon the differentiation. Once calculated, all partial derivatives were inserted into the Hessian matrix in Equation (2).

IX. REFERENCES

Bergmark, A., 1989. Stability of the lumbar spine. A study in mechanical engineering. Acta Orthopaedica Scandinavica 230 (Suppl.), 1-54.

Brown, S.H., Potvin, J.R., 2005. Constraining spine stability levels in an optimization model leads to the prediction of trunk muscle cocontraction and improved spine compression force estimates. Journal of Biomechanics 38, 745-754.

Callaghan, J.P., McGill, S.M., 1995. Muscle activity and low back loads under external shear and compressive loading. Spine 20, 992-998.

Cholewicki, J., McGill, S.M., 1992. Lumbar posterior ligament involvement during extremely heavy lifts estimated from fluoroscopic measurements. Journal of Biomechanics 25, 17-28.

Cholewicki, J., McGill, S.M., Norman, R.W., 1995. Comparison of muscle forces and joint load from an optimization and EMG assisted lumbar spine model: towards development of a hybrid approach. Journal of Biomechanics 28, 321-331.

Cholewicki, J., McGill, S.M., 1995. Relationship between muscle force and muscle stiffness in the whole mammalian muscle: A simulation study. Journal of Biomechanical Engineering 117, 339-342.

Cholewicki, J., McGill, S.M., 1996. Mechanical stability of the in vivo lumbar spine: Implications for injury and chronic low back pain. Clinical Biomechanics 11, 1-15.

Cholewicki, J., Juluru, K., McGill, S.M., 1999. Intra-abdominal pressure mechanism for stabilizing the lumbar spine. Journal of Biomechanics 32, 13-17.

Cholewicki, J., Simons. A.P.D.,Radebold, A., 2000. Effects of external trunk loads on lumbar spine stability. Journal of Biomechanics 33, 1377-1385.

Cholewicki, J., VanVliet IV, J.J., 2002. Relative contributions of trunk muscles to the stability of the lumbar spine during isometric exertions. Clinical Biomechanics 17, 99-105.

Crisco, J.J., Panjabi, M.M., 1992. Euler stability of the human ligamentous lumbar spine. Part I: Theory. Clinical Biomechanics 7, 19-26.

Crisco, J.J., Panjabi, M.M., Yamamoto, I., Oxland, T.R., (1992). Euler stability of the human ligamentous lumbar spine. Part II: Experiment. Clinical Biomechanics 7, 27-32.

Farfan, H.F., Gracovetsky, S., 1984. The nature of instability. Spine 9, 714-719.

Farshad, M., 1994. Stability of structures. Elsevier, Netherlands.

Gardner-Morse, M., Stokes, I.A.F., Laible, J.P., 1995. Role of muscles in lumbar spine stability in maximum extension efforts. Journal of Orthopaedic Research 13, 802-808.

Granata, K.P., Marras, W.S., 2000. Cost-benefit of muscle cocontraction in protecting against spinal instability. Spine 25, 1398-1404.

Granata, K.P., Orishimo, K.F., 2001. Response of trunk muscle coactivation to changes in spinal stability. Journal of Biomechanics 34, 1117-1123.

Hodges, P.W., Richardson, C.A., 1997. Feedforward contraction of transverse abdominis is not influenced by the direction of arm movement. Experimental Brain Research 114, 362-370.

Hodges, P.W., Eriksson, A.E.M., Shirley, D., Gandevia, S.C., 2005. Intra-abdominal pressure increases stiffness of the lumbar spine. Journal of Biomechanics 38, 1873-1880.

Howarth, S.J., Allison, A.E., Grenier, S.G, Cholewicki, J., McGill, S.M., 2004. On the implications of interpreting the stability index: A spine example. Journal of Biomechanics 37, 1147-1154.

Howarth, S.J., McGill, S.M., 2005. Using the eigenvector approach to locate spinal instability. Proceedings of the XXth Congress of the International Society of Biomechanics, Cleveland, Ohio, July 31 - August 5.

Kaigle, A.M., Holm, S.H., Hansson, T.H., 1995. Experimental instability in the lumbar spine. Spine 20, 421-430.

Kavcic, N., Grenier, S., McGill, S.M., 2004. Determining the stabilizing role of individual torso muscles during rehabilitation exercises. Spine 11, 1254-1265.

MacDonald, D.A., Moseley, G.L., Hodges, P.W., 2006. The lumbar multifidus muscle: Does the evidence support clinical beliefs? Manual Therapy, in press.

McGill, S.M., Norman, R.W., 1986. Partitioning of the L4-L5 dynamic moment into disc, ligamentous, and muscular components during lifting. Spine 11, 666-678.

McGill, S.M., Seguin, J., Bennett, G., 1994. Passive stiffness of the lumbar torso in flexion, extension, lateral bending, and axial rotation. Effect of belt wearing and breath holding. Spine 19, 696-704.

McGill, S.M., 2001. Low back stability: From formal description to issues for performance and rehabilitation. Exercise and Sport Science Reviews 29, 26-31.

McGill, S., 2002. Low back disorders. Evidence based prevention and rehabilitation. Human Kinetics, Illinois.

McGill, S.M., Grenier, S., Kavcic, N., Cholewicki, J., 2003. Coordination of muscle activity to assure stability of the lumbar spine. Journal of Electromyography and Kinesiology 13, 353-359.

Oxland, T.R., Panjabi, M.M., Southern, E.P., Duranceau, J.S., 1991. An anatomic basis for spinal instability: A porcine trauma model. Journal of Orthopaedic Research 9, 452-462.

Oxland, T.R., Panjabi, M.M., 1992. The onset and progression of spinal injury: A demonstration of neutral zone sensitivity. Journal of Biomechanics 25, 1165-1172.

Panjabi, M.M., Abumi, K., Duranceau, J., Oxland, T., 1989. Spinal stability and intersegmental muscle forces: A biomechanical model. Spine 14, 194-199.

Panjabi, M.M., Kifune, M., Liu, W., Arand, M., Vasavada, A., Oxland, T.R., 1998. Graded thoracolumbar spinal injuries: Development of multidirectional instability. European Spine Journal 7, 332-339.

Panjabi, M.M., 2003. Clinical spinal instability and low back pain. Journal of Electromyography and Kinesiology 13, 371-379.

Pope, M.H., Panjabi, M., 1985. Biomechanical definitions of spinal instability. Spine 10, 255-256.

Posner, I., White, A.A., Edwards, W.T., Hayes, W.C., 1982. A biomechanical analysis of the clinical stability of the lumbar and lumbosacral spine. Spine 7, 374-389.

Potvin, J.R., Brown, S.H., 2005. An equation to calculate individual muscle contributions to joint stability. Journal of Biomechanics 38, 973-980.

Scannell, J.P., McGill, S.M., 2003. Lumbar posture – should it, and can it be modified? A study of passive tissue stiffness and lumbar position during activities of daily living. Physical Therapy 83, 907-917.

Stokes, I.A.F., Gardner-Morse, M., 1994. Lumbar spine maximum efforts and muscle recruitment patterns predicted by a model with multijoint muscles and joints with stiffness. Journal of Biomechanics 28, 173-186.

Stokes, I.A.F., Gardner-Morse, M., 2003. Spinal stiffness increases with axial load: another stabilizing consequence of muscle action. Journal of Electromyography and Kinesiology 13, 397-402.

Thompson, J.M., Hunt, G.W., 1984. Elastic Instability Phenomena. Wiley, New York.

Ulrich, Q., Wilke, H-J., Shirazi-Adl, A., Pamianpour, M., Loer, F., Claes, L., 1998. Importance of the intersegmental trunk muscles for the stability of the lumbar spine: A biomechanical study in vitro. Spine 23, 1937-1945.

van Dieen, J.H., Cholewicki, J., Radebold, A., 2003. Trunk muscle recruitment patterns in patients with low back pain enhance the stability of the lumbar spine. Spine 28, 834-841.

Wilke, H.J., Wolf, S., Claes, L.E., Arand, M., Wiesend, A., 1995. Stability increase of the lumbar spine with different muscle groups. A biomechanical in vitro study. Spine 20, 192-198.

Wu, G., Siegler, S., Allard, P., Kirtley, C., Leardini, A., Rosenbaum, D., Whittle, M., D'Lima, D.D., Cristofolini, L., Witte, H., Schmid, O., Stokes, I., 2002. ISB recommendation on definitions of joint coordinate system of various joints for the reporting of human joint motion--part I: ankle, hip, and spine. International Society of Biomechanics. Journal of Biomechanics 35, 543-548.